Keynote Paper

ANALYTICAL METHOD IN INVERSE HEAT TRANSFER PROBLEM USING LAPLACE TRANSFORM TECHNIQUE
Application to one- and two-dimensional cases

Masanori Monde*, Hirofumi Arima, Wei Liu and Yuhichi Mitsutake
Department of Mechanical Engineering, Saga University
1 Honjo, Saga, 840- 8502, JAPAN

Abstract An analytical method has been developed for the inverse problem in one- and two-dimensional heat conduction, when the temperatures are known at an appropriate number of the measuring points. On the basis of these known temperatures, a closed form solution is determined for the transient temperatures by using Laplace transform technique. This method first approximates the temperature data with a half polynomial power series of time. The resultant expression for an objective temperature and heat flux are explicitly obtained in the form of power series of time. Numerical results for some representative problems show that the surface temperature and heat flux can be predicted for not only one- but also two-dimensional heat conductions well by the present method.

Keywords: Inverse solution, Heat conduction, Analytical solution, Laplace Transformation.

INTRODUCTION

A procedure to solve inverse heat transfer problem (IHTP) is very important in determining unknown surface temperature and heat flux from known values in the body, which are usually measured as a function of space and time. Especially, under the severe surface conditions such as reentry of space vehicle and an accident involving coolant breaks in the plasma-facing components, a direct measurement of the heat flux or temperature change on the surface is almost impossible so that the prediction of these values cannot help depending on the solution of IHTP. In addition, several studies about IHTP have been carried out to predict the transient surface conditions during quenching a hot body. Recently, the IHTP has been numerically treated and extended to multiple dimensions with help of development of computing architecture and improvement of computer capacities. Several approaches about the IHTP (Alifanov, 1994 and Beck, 1985) are summarized. Nevertheless, a theoretical method using Laplace transformation has been still interesting when the configurations involved are rather simple such as rectangular and cylindrical shapes and then the known boundary conditions are not complicated, since the solution to the IHTP can be explicitly derived predicting the surface conditions with a simple functional form. As an example of analytical method of one dimensional IHTP, a procedure using an exact solution by Buggraf (1964) and a method using Duhamel solution and Laplace transformation are widely used. Shoji (1978) pointed out earlier that Laplace transformation is promising in treating one dimensional IHTP. Imber (1974) and Imber and Khan (1972) extended a procedure using Laplace transformation for one dimensional IHTP to one for two and three dimensional IHTPs, since it is relatively simple to extend two and three dimensional IHTPs for the case that the geometrical configurations involved are not complicated. As for numerical method, Heieh and Su (1980), Bell (1984) and Lithouhi and Beck (1986) solved two dimensional IHTP based on finite different method, while Shoji and Ono (1988) based on boundary element method. Huang and Tsai (1998) carried out an analysis to arbitrary boundary problem by using conjugate gradient method. Frankel et al. (1997) first approximated the temperature change at a point using polynomial series of Cheviseff, and then gave the solution of IHTP by determining each coefficient of polynomial series in order to minimize a weighted residual in the governing equation. Recently, Monde (2000), Monde et al. (2000) and Arima et al. (2001) have succeeded in getting an analytical solution for one-dimensional heat conduction using the Laplace transformation and shows that the surface temperature or the surface heat flux can be predicted accurately and easily by using the analytical solution. The reason that the Monde method prefers to the Shoji (1978) and Imber (1974) ones, is that an approximate function employs half polynomial series of time and take into account of a time lag, and it is applicable for an initial temperature distribution in a solid. It should be mentioned finally that Monde and Mitsutake (2001) proposed a new method based on success of this analytical inverse solution which makes it possible to measure thermal diffusivity and thermal conductivity

*Email:monde@me.saga-u.ac.jp

more accurate and easier than that based on a direct solution.

More recently, Monde et al. (2001) have applied his method to two-dimensional case and derived an inverse solution of heat conduction in finite rectangular coordinate, showing that a good estimation of the surface temperature as well as the surface heat flux were obtained.

The objective of this paper is to review our recent study of inverse problem in one- and two-dimensional heat conductions.

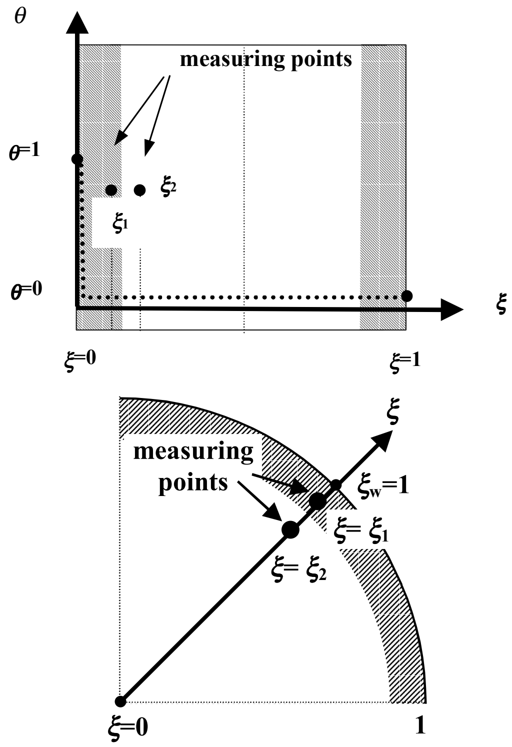

Fig. 1 Sketch illustrating inverse heat conduction problem for one measuring point

ANALYSIS OF ONE DIMENSIONAL HEAT CONDUCTION

One-dimensional heat conduction equation with constant properties and no internal heat generation in a solid as shown in Fig.1 can be written in a non-dimensional form as:

$$\frac{\partial \theta}{\partial \tau} = \frac{1}{\xi^{\kappa}}\left(\frac{\partial}{\partial \xi}\xi^{\kappa}\frac{\partial \theta}{\partial \xi}\right) \quad (1)$$

where, $\kappa = 0$ corresponds to rectangular coordinate, $\kappa = 1$ to cylindrical one, $\kappa = 2$ to spherical one. For an initial condition of $\theta = \theta_0(\xi)$, Laplace transformation of Eq. (1) becomes as:

$$\frac{1}{\xi^{\kappa}}\frac{d}{d\xi}\left(\xi^{\kappa}\frac{d\bar{\theta}}{d\xi}\right) - p^2\bar{\theta} = -\theta_0 \quad (2)$$

It is possible to treat with Eq. (2) for rectangular or cylindrical or spherical coordinate depending on $\kappa = 0$, 1 or 2. However, the case for rectangular coordinate namely $\kappa = 0$ only will be discussed here, and the other cases will be briefly written due to a limited space.

Initial Temperature Distribution

The temperature in the solid has been in a steady state where $\partial\theta / \partial\tau = 0$, before transient heat conduction will start. Therefore, the initial temperature distribution in the solid with heat generation of q_0 can be generally given for three different coordinates by the following equation.

$$\frac{\partial^2 \theta}{\partial \xi^2} = q_0 \quad (3)$$

The initial temperature distribution can be easily given by a quadratic function as:

$$\theta_0(\xi) = a_0 + a_1\xi + a_2\xi^2 \quad (4)$$

The three constants of a_0, $a_1$and a_2 are determined from a given steady state condition.

General Solution

The general solution of Eq. (2) with initial temperature distribution, $\theta_0(\xi)$, can be easily given as:

$$\bar{\theta}(\xi, s) = Ae^{-p\xi} + Be^{p\xi} + \frac{\theta_0(\xi)}{s} + \frac{2a_2}{s^2} \quad (5)$$

where $p^2 = s$, and s is Laplace's operator and A, B are integral constants subject to surface conditions.

Solution for Finite Body

In the case of IHTP for a finite plane, two known temperatures in the plate are necessary at least to close Eq.(5). Therefore, let the two temperatures at two different points of $\xi = \xi_1$, ξ_2 ($\xi_1 < \xi_2$) be as:

$$\bar{\theta}(\xi_n, s) = \bar{f}_n(s), \quad n = 1, 2 \quad (6)$$

Substitution of Eq. (6) in Eq. (5) gives

$$\bar{f}_n(s) = Ae^{-p\xi_n} + Be^{p\xi_n} + \frac{\theta_0(\xi_n)}{s} + \frac{2a_2}{s^2}, \quad n = 1, 2 \quad (7)$$

After determining the constants of A, B in Eq. (7) and then substituting the values of A, B into Eq.(5), we can obtain the temperature in the body as follows:

$$\bar{\theta}(\xi,s) = \frac{\bar{f}_1(s)\sinh\{p(\xi_2-\xi)\} - \bar{f}_2(s)\sinh\{p(\xi_1-\xi)\}}{\sinh\{p(\xi_2-\xi_1)\}} - \frac{(\theta_0(\xi_1)/s+2a_2/s^2)\sinh\{p(\xi_2-\xi)\}}{\sinh\{p(\xi_2-\xi_1)\}} + \frac{(\theta_0(\xi_2)/s+2a_2/s^2)\sinh\{p(\xi_1-\xi)\}}{\sinh\{p(\xi_2-\xi_1)\}} + \frac{\theta_0(\xi_n)}{s} + \frac{2a_2}{s^2} \quad (8)$$

and the surface temperature can be easily obtained by setting $\xi = 0$ as:

$$\bar{\theta}_w(s) = \frac{\bar{f}_1(s)\sinh(p\xi_2) - \bar{f}_2(s)\sinh(p\xi_1)}{\sinh\{p(\xi_2-\xi_1)\}} - \frac{(\theta_0(\xi_1)/s+2a_2/s^2)\sinh(p\xi_2)}{\sinh\{p(\xi_2-\xi_1)\}} + \frac{(\theta_0(\xi_2)/s+2a_2/s^2)\sinh(p\xi_1)}{\sinh\{p(\xi_2-\xi_1)\}} + F_1(a_0,a_2,s) \quad (9)$$

Likewise, the solution for the heat flux can be also obtained as:

$$\bar{\Phi}(\xi,s) = p\frac{\bar{f}_1(s)\cosh\{p(\xi_2-\xi)\} - \bar{f}_2(s)\cosh\{p(\xi_1-\xi)\}}{\sinh\{p(\xi_2-\xi_1)\}} - p\frac{(\theta_0(\xi_1)/s+2a_2/s^2)\cosh\{p(\xi_2-\xi)\}}{\sinh\{p(\xi_2-\xi_1)\}} + p\frac{(\theta_0(\xi_2)/s+2a_2/s^2)\cosh\{p(\xi_1-\xi)\}}{\sinh\{p(\xi_2-\xi_1)\}} - 2\frac{a_2}{s}\xi - \frac{a_1}{s} \quad (10)$$

where, $\bar{\Phi}(\xi,s) = -\partial\bar{\theta}(\xi,s)/\partial\xi\big|_{\xi=0}$

The surface heat flux becomes,

$$\bar{\Phi}_w(s) = \frac{p\bar{f}_1(s)\cosh(p\xi_2) - p\bar{f}_2(s)\cosh(p\xi_1)}{\sinh\{p(\xi_2-\xi_1)\}} - \frac{(\theta_0(\xi_1)/s+2a_2/s^2)p\cosh(p\xi_2)}{\sinh\{p(\xi_2-\xi_1)\}} + \frac{(\theta_0(\xi_2)/s+2a_2/s^2)p\cosh(p\xi_1)}{\sinh\{p(\xi_2-\xi_1)\}} + G_1(a_1,s) \quad (11)$$

where, $F_1(a_0, a_2, s)$ and $G_1(a_1, s)$ are function of initial temperature distributions (see Appendix I)

Approximate Equation for Temperature at a Measuring Point

In order to perform inverse Laplace transformation of Eqs. (9) and (11), we first have to give the known functions, $\overline{f_n}(s)$, @$n = 1,2$ included in $\bar{\theta}_w(s)$ and $\bar{\Phi}_w(s)$, explicitly. By the way, the subsidiary function of $f_n(\tau)$ can be determined so as to approximate temperature changes at two different measuring points of $\xi = \xi_1$ and ξ_2, respectively.

Any function $f_n(\tau)$ is available in approximating the temperature change. Therefore, Monde (2000) tried some different kinds of functions on which the something of IHTP depends and finally recommended half polynomial series of time with a time lag as given by Eq. (12), since Eq. (12) can give the best estimation among them.

$$f_n(\tau) = \sum_{k=0}^{N}\frac{b_{k,n}}{\Gamma(k/2+1)}(\tau-\tau_n^*)^{\frac{k}{2}}, \quad n = 1, 2 \quad (12)$$

where, coefficients $b_{k,n}$ can be determined by using, for example, the least mean square method from the measured temperature and N gives number of terms of polynomial series. This time lag τ_n^* can be determined from *erfc* $(\xi_n/2\sqrt{\tau_n})$ = min (θ). The reason why polynomial series of time is recommended is that a general solution for one dimensional heat conduction is provided in functional form of $\theta = (\xi/\sqrt{\tau})$

The subsidiary form of Eq. (12) is easily obtained as:

$$\bar{f}_n(s) = e^{-s\tau_n^*}\sum_{k=0}^{N} b_{k,n}/s^{(k/2+1)} \quad n = 1, 2 \quad (13)$$

After substituting Eq. (13) into Eqs. (9) and (11), one performs inverse Laplace transformation to give the surface temperature and heat flux. However, even if one performs this inverse transformation exactly, we can only know the estimated solution of surface temperature and heat flux for $\tau > \tau_{min}$, because the solution always diverges as $\tau \to 0$. Therefore, in order to follow another way rather than direct inverse Laplace transformation of Eqs. (9) and (11) , we first expand hyperbolic functions in Eqs. (9) and (11) in a series around $s = 0$, and then perform inverse Laplace transformation to obtain the approximate solutions (Monde, 2000).

Approximate Equation of Inverse Problem Solution

The approximate equations for surface temperature and heat flux can be obtained by performing inverse Laplace transformation of Eqs. (9) and (11) as:

$$\theta_w(\tau) = \sum_{j=-1}^{N} C_{j,12}(\tau-\tau_1^*)^{j/2}/\Gamma(\frac{j}{2}+1) - \sum_{j=-1}^{N} C_{j,21}(\tau-\tau_2^*)^{j/2}/\Gamma(\frac{j}{2}+1) + W(a_2) \quad (14)$$

$$\Phi_w(\tau) = \sum_{j=-1}^{N} D_{j,12}(\tau-\tau_1^*)^{j/2}/\Gamma(\frac{j}{2}+1) - \sum_{j=-1}^{N} D_{j,21}(\tau-\tau_2^*)^{j/2}/\Gamma(\frac{j}{2}+1) + Y(a_2) \quad (15)$$

The coefficients of $C_{j,12}$, $C_{j,21}$, $D_{j,12}$, $D_{j,21}$, $W(a_2)$, $Y(a_2)$ in Eqs. (14) and (15) are listed in Appendices I and II. When we set $a_2 = 0$, all coefficients of $W(a_2)$ and $Y(a_2)$ become 0. Then, Eqs. (14) and (15) become the approximate ones for the initial temperature distribution θ_0 being constant (or 0). In other words, the approximate equation for the initial temperature with linear temperature distribution is the same as that with constant temperature distribution.

It should be noted that the initial temperature distribution has been held in the finite plane but it is never held in the semi-infinite body. Therefore, the effect of initial temperature condition is not necessary to be discussed.

Procedure to Solution in Cylindrical and Spherical Coordinates

How to obtain the inverse solutions in cylindrical and spherical coordinates are explained here briefly, since they are identical to the method for rectangular case.

The initial temperature distributions at a steady state can be expressed in cylindrical and spherical coordinates as:

$$\theta_0(\xi) = a_0 + a_1 \ln \xi + a_2 \xi^2 \tag{16}$$

$$\theta_0(\xi) = a_0 + a_1 / \xi + a_2 \xi^2 \tag{17}$$

And the inverse solutions of surface temperature and heat flux on cylindrical coordinate can be expressed as,

$$\begin{aligned}\bar{\theta}_w &= \bar{f}_1(s)K_{1,2}(s) - \bar{f}_2(s)K_{1,1}(s) - (\theta_0(\xi_1)/s + 4a_2/s^2)K_{1,2}(s) \\ &+ (\theta_0(\xi_2)/s + 4a_2/s^2)K_{1,1}(s) + F_2(a_0, a_2, s)\end{aligned} \tag{18}$$

$$\begin{aligned}\bar{\Phi}_w &= \bar{f}_1(s)K_{2,2}(s) - \bar{f}_2(s)K_{2,1}(s) - (\theta_0(\xi_1)/s + 4a_2/s^2)K_{2,2}(s) \\ &+ (\theta_0(\xi_2)/s + 4a_2/s^2)K_{2,1}(s) + G_2(a_1, a_2, s)\end{aligned} \tag{19}$$

where, $K_{1,1}$(s), $K_{1,2}$(s), $K_{2,1}$(s), $K_{2,2}$(s) are called "the kernels" of Eqs. (18) and (19) (See Appendix II), the functions of $F_2\,(a_0, a_2, s)$ and $G_2\,(a_1, a_2, s)$ are related to the initial temperature.

For spherical coordinate, likewise, the surface temperature and heat flux are also expressed as:

$$\begin{aligned}\bar{\theta}_w &= \bar{f}_1(s)K_{1,2}(s) - \bar{f}_2(s)K_{1,1}(s) - (\theta_0(\xi_1)/s + 6a_2\xi_1/s^2)K_{1,2}(s) \\ &+ (\theta_0(\xi_2)/s + 6a_2\xi_2/s^2)K_{1,1}(s) + F_3(a_0, a_1, a_2, s)\end{aligned} \tag{20}$$

$$\begin{aligned}\bar{\Phi}_w &= \bar{f}_1(s)K_{2,2}(s) - \bar{f}_2(s)K_{2,1}(s) - (\theta_0(\xi_1)/s + 6a_2\xi_1/s^2)K_{2,2}(s) \\ &+ (\theta_0(\xi_2)/s + 6a_2\xi_2/s^2)K_{2,1}(s) + G_3(a_1, a_2, s)\end{aligned} \tag{21}$$

where, $K_{1,1}$(s), $K_{1,2}$(s), $K_{2,1}$(s), $K_{2,2}$(s) are the kernels (See the Appendix II) and the functions of $F_3\,(a_0, a_1, a_2, s)$ and $G_3\,(a_1, a_2, s)$ are related to the initial temperature.

Approximate Inverse Solution for Cylindrical and Spherical Coordinates

The approximate equations for the surface temperature and the heat flux are obtained by performing the inverse transformation on Eqs. (18) and (19) for cylindrical coordinate and Eqs. (20) and (21) for spherical coordinate, which are in a similar form of Eqs. (14) and (15). Each coefficient of $C_{j,12}$, $C_{j,21}$, $D_{j,12}$, $D_{j,21}$, W and Y is listed in Appendices I and II.

When we replace $W(a_2)$ and $Y(a_2)$ by $W_c(a_2)$ and $Y_c(a_2)$ for cylindrical coordinate and by $W_s(a_2)$ and $Y_s(a_2)$ for spherical coordinate, respectively, and let $a_2 = 0$, then all coefficients of $W_c(a_2)$, $Y_c(a_2)$, $W_s(a_2)$ and $Y_s(a_2)$ become 0 like rectangular coordinate. It is worth mentioning finally that the inverse solutions for constant initial and linear temperature distributions become identical.

Characteristic of Inverse Solution in Cylindrical and Spherical Coordinates

In case of treating with the temperature change for $0 \le \xi < 1$ in cylindrical and spherical coordinates, the boundary condition at $\xi = 0$ always becomes $\partial\theta/\partial\xi = 0$. Therefore, number of measuring point included in Eqs. (18) and (19) and Eqs. (20) and (21) is reduced to one.

Consequently, these inverse solutions thereby become simpler than Eqs. (18) and (19) and also Eqs. (20) and (21), but predict worse estimation than those. The reason is that even though the boundary condition of $\partial\theta/\partial\xi = 0$ is exact, this point is the furthest from the other surface. Therefore, according to Monde (2000), it is of significance to choose the measuring point as close to surface as possible for getting better estimations from the measured temperature.

As for these problems, how the approximate solution is influenced by position of temperature measurement will be discussed later.

Approximate Solution for Semi-Infinite Body

General solution for semi-infinite body is easily obtained by setting $A = 0$, $a_1 = a_2 = 0$ in Eq. (5), since there is no initial temperature distribution in it at steady state. The finite and semi-infinite plates are different in number of unknown variables, the former has one and the latter has two. Therefore, one measuring point is enough for semi-infinite plate. Now, when the temperature distribution is given by, for example, Eq. (12) at $\xi = \xi_1$, one can determine the representative function of unknown constant B. The equations for surface temperature and heat flux can be given as follows:

$$\bar{\theta}_w(\tau) = \frac{1}{2\pi i}\int_{c-i\infty}^{c+i\infty} e^{s(\tau-\tau_1^*)} e^{p\xi_1} \sum_{k=0}^{N} b_{k,1} / s^{(\frac{k}{2}+1)} ds \tag{22}$$

$$\bar{\Phi}_w(\tau) = \frac{1}{2\pi i}\int_{c-i\infty}^{c+i\infty} e^{s(\tau-\tau_1^*)} p e^{p\xi_1} \sum_{k=0}^{N} b_{k,1} / s^{(\frac{k}{2}+1)} ds \tag{23}$$

We first expand the integrand $e^{p\xi_1}$ in a series around $s = 0$, and then we perform inverse Laplace transformation to give the surface temperature and heat flux as:

$$\theta_w(\tau) = \sum_{j=-1}^{N} U_j (\tau - \tau_1^*)^{j/2} / \Gamma(\frac{j}{2}+1) \tag{24}$$

$$\Phi_w(\tau) = \sum_{j=-1}^{N} V_j (\tau - \tau_1^*)^{j/2} / \Gamma(\frac{j}{2}+1) \tag{25}$$

Semi-infinite body can be also assumed in cylindrical and spherical coordinates, but we did not consider this case, since it is seldom used in engineering field.

PROCEDURE TO DETERMINE COEFFICIENTS IN EQ. (12)

The coefficient, $b_{k,n}$, in Eq. (12) can be determined from the measured temperature, for example, by the least mean square method. Then the coefficients are greatly subject to significant digit of the data or precision of measured values, what level of data's accuracy is used is important. Generally speaking, the measured temperature includes some uncertainty. Therefore, the simulated measuring temperature calculated from the exact solution can be expressed as:

$$\theta(\xi_n,\tau) = \theta_{exact}(\xi_n,\tau)(1+0.005\varepsilon) \text{ @, } n = 1, 2 \tag{26}$$

where, θ_{exact} (ξ_n,τ) is the exact solution for the corresponding boundary condition, and m and σ are average and standard deviation for a random value of ..respectively. It should be noted to remember that accuracy in a temperature measured by using thermocouple would be generally expected to be a significant digit of 2 or 3.

There is another method except for Eq. (26), which is cut-off to the second decimal place, but it is commonly way to employ Eq. (26) in which a certain disturbance is superposed on the exact solution. It was reported (Monde, 2000) the solution obtained by Eq. (26) is worse approximation than by cut-off method.

Figure 2 shows the temperature response measured at a point and the approximate curves given by Eq. (12) with a different value of N. From Fig. 2, the approximated solution is improved with an increase in N, but it would be saturated around N = 5 ~ 7 beyond which the improvement is not expected greatly. Therefore, the order of approximate equation can be considered to be N = 7 at most.

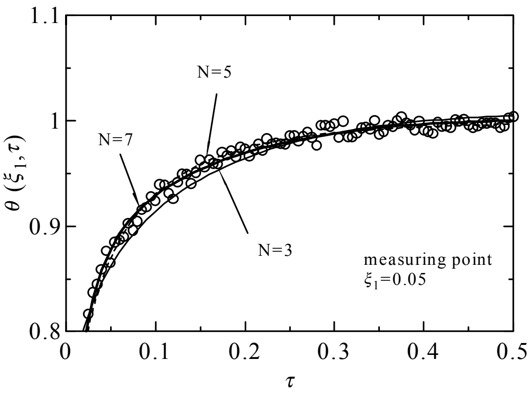

Fig. 2 Approximate curve for temperature change at a point

INVERSE SOLUTION AND REPRESENTATIVE PROBLEMS

Method for Calculation

The procedure to solve inverse problems is:

1. Determine each coefficient of $b_{k,n}$ in Eq. (12) obtained from the temperature at the point of ξ_1 or ξ_2 by the least mean square method.
2. Expand the kernels of solution obtained by performing Laplace transformation around s = 0 in a series in which the coefficients are summarized in Appendix II.
3. Calculate coefficients given by multiplying coefficients in Eq. (12) and the coefficients of the kernel, which are summarized in Appendix II.
4. Perform inverse Laplace transformation, and calculate explicitly the surface temperature and heat flux using Eqs. (14) and (15), (18) and (19), (20) and (21).

Representative Problems

The approximating solutions for several boundary conditions are reported by Monde (2000), Monde et al. (2000). We here, investigate about five representative combinations of initial temperature distributions and boundary conditions as listed in Table 1, which were not included in the papers of Monde (2000), and Monde et al. (2000).

Inverse Solution Calculated

Figures 3 (a) to (d) show comparisons between the exact solution of surface temperatures and the corresponding estimated solutions for the cases 1, 2, 4 and 5. Figures 4 (a) and (b) show comparisons between the exact solutions of heat flux and corresponding estimated ones. The value of N in Figs. 3 (a) to (d) and Figs. 4 (a) to (b) means the order of approximate equation and the values of ξ_1 and ξ_2 corresponding to the position of the measuring point in the solid. And, the temperatures at each measuring point were obtained by Eq. (26). Figures 3 and 4 show that the estimated solutions approach to the exact solution with increase in the value of *N*.

Table 1 Boundary condition and exact solution (For all cases, finite body)

Case	Boundary condition ($0<\tau$)	Parameters
1 (1st B.C.)	$\theta(\tau)=1:\ \xi=0$ $\theta(\tau)=0:\ \xi=1$ $\theta=0:\ \tau=0$	$\theta=T/T_0$ $\Phi=qL/\lambda T_0$
2 (1st B.C.)	$\theta(\tau)=\tau:\ \xi=0$ $\theta(\tau)=0:\ \xi=1$ $\theta=0:\ \tau=0$	$\theta=T/T_0$ $\Phi=qL/\lambda T$
3 (2nd B.C.)	$\Phi(\tau)=1:\ \xi=0$ $\Phi(\tau)=0:\ \xi=1$ $\theta=0:\ \tau=0$	$\theta=T\lambda/q_0L$ $\Phi=q/q_0$
4 (3rd B.C.)	$\frac{\partial\theta}{\partial\xi}=\mathrm{Bi}(\theta-\theta_\infty(\tau))$, $\theta_\infty(\tau)=1:\ \xi=0$ $\frac{\partial\theta}{\partial\xi}=0:\ \xi=1$ $\theta=0:\ \tau=0$	$\theta=T/T_0$ $\Phi=qL/\lambda T_0$
5 (1st B.C. with I.C.)	$\theta(\tau)=1:\ \xi=0$ $\theta(\tau)=0:\ \xi=1$ $\theta=\xi^2:\ \tau=0$	$\theta=T/T_0$ $\Phi=qL/\lambda T_0$

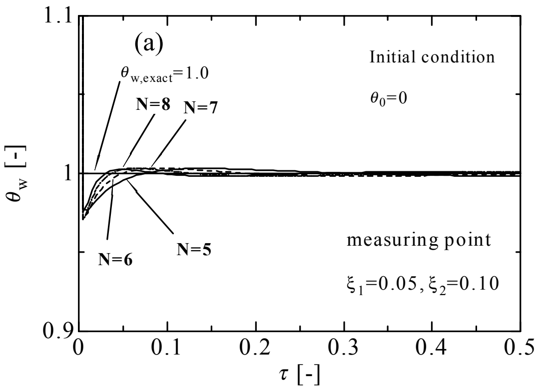

(a) Case 1

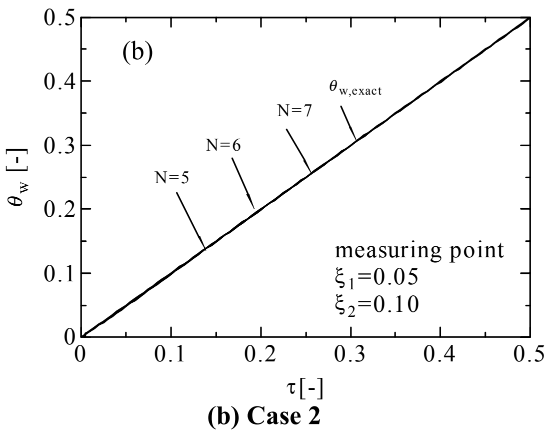

(b) Case 2

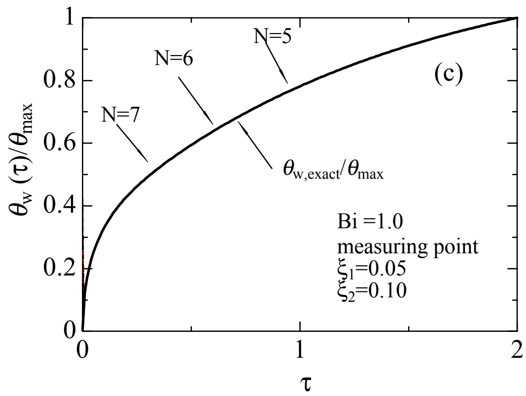

(c) Case 4

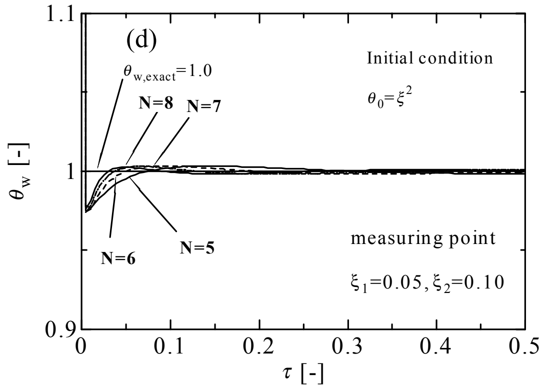

(d) Case 5

Fig. 3 Estimated surface temperature for (a) Case 1, (b) Case 2, (c) Case 4 and (d) Case 5

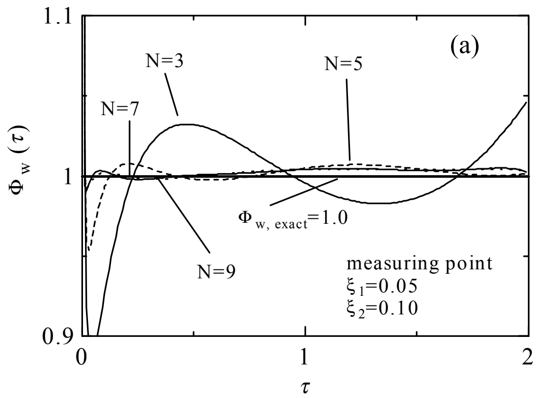

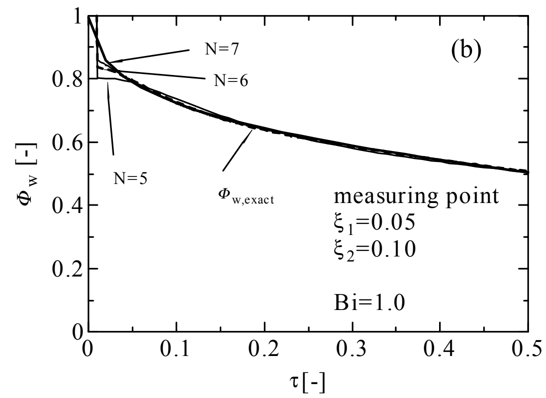

Fig. 4 Estimated surface heat flux for (a) Case 3 and (b) Case 5

EVALUATION OF ESTIMATED VALUE

Minimum Predictive Time

It is mathematically proved (Alifanov, 1994 and Beck, 1985) that no inverse solution exists at $\tau = 0$ and the solution can converge beyond a limiting time. Therefore, a minimum predictive time is an important factor in evaluating the inverse solution. One may adopt the minimum predictive time, τ_1 at which inverse solution first satisfies within a relative difference of 0.01 (error is less than 1 %) between the exact and the estimated values and from which the solution is validated. Table 2 shows the minimum predictive time for every cases against the value of *N*. It is found from Table 2 that the minimum predictive time is hardly influenced except for cases 3 and 4 by the value of *N*. However, in the cases 3 and 4, the value of *N* larger than 5 does not almost influence the minimum predictive time.

Table 2 Minimum initial time (τ_1) estimated for error of 0.01 for ξ_1 = 0.05, ξ_2 = 0.10 (initial condition; $\theta = 0$)

N	case1	case2	case3	case4	case5
3	0.0050	0.0057	0.0233	0.0093	0.0050
4	0.0050	0.0057	0.0317	0.0067	0.0050
5	0.0050	0.0056	0.0189	0.0074	0.0050
6	0.0050	0.0047	0.0093	0.0051	0.0050
7	0.0050	0.0076	0.0059	0.0050	0.0050
8	0.0051	0.0057	0.0056	0.0050	0.0051

Table 3 Standard deviation (σ) (initial condition; $\theta = 0$)

N	case1	case2	case3	case4	case5
3	0.0029	0.0091	0.0050	0.0056	0.0030
4	0.0030	0.0093	0.0020	0.0016	0.0032
5	0.0031	0.0093	0.0018	0.0012	0.0024
6	0.0029	0.0093	0.0008	0.0007	0.0029
7	0.0026	0.0094	0.0005	0.0002	0.0025
8	0.0022	0.0094	0.0005	0.0002	0.0013

Accuracy of Estimation

In order to evaluate the accuracy of the inverse solution, we introduce standard deviation as:

$$\sigma = \sqrt{\frac{1}{(\tau_2 - \tau_1)} \int_{\tau_1}^{\tau_2} (\theta_{w,exact}(\tau) - \theta_{w,cal}(\tau))^2 d\tau}$$

where τ_2 is defined as 90 % of the end time of the measurement since its time was chosen to avoid an effect of the end time on the estimated temperature. Table 3 shows that the minimum standard deviation of σ = 0.003 appears at *N* = 6 beyond which the accuracy of prediction is not expected to improve any more. Taking into account the fact that the deviation in prediction reaches the same level as deviation of approximate equation, we cannot expect more accuracy in this method. In addition, it is found from Table 3 that the approximate equation at the order of *N* = 6 gives the most accurate solution.

Estimated Solution of Surface Heat Flux

It is concluded from Figs. 4 (a) and (b) that the inverse solutions for the surface heat flux obtained by using *N* = 5 to 7 in Eq. (15) also agree well with the exact ones.

Effect of Position of Temperature Measurement on Estimated Solution

Figure 5 shows an effect of the position of the temperature measurement on the inverse solution for the case 3 when using *N* = 5. The position of ξ_2 = 0.5 in Fig. 5 corresponds to the farthest point from the surface in a finite body.

According to Fig. 5, the inverse solution for ξ_1 = 0.05 and 0.1 are in good agreement with the exact value, although for a ξ_1 = 0.2 and 0.3, both the solutions and the time are not recommended because of a large deviation and delayed time.

On the other hands, the accuracy of prediction on these conditions is still the same as that for ξ_1= 0.05 and ξ_2 = 0.1 as shown in Fig. 3 (a) and Table 2, but the minimum predictive time becomes larger than that forξ_1= 0.05 and ξ_2 = 0.1.

Consequently, it may be recommended to choose the measuring points as close to the surface as possible to give a good estimation. In particular, the point ξ_1 is recommended to be $\xi_1 < 0.1$. On the other hand, we may recommend $\xi_1 \leq 0.2$ for the minimum prediction time.

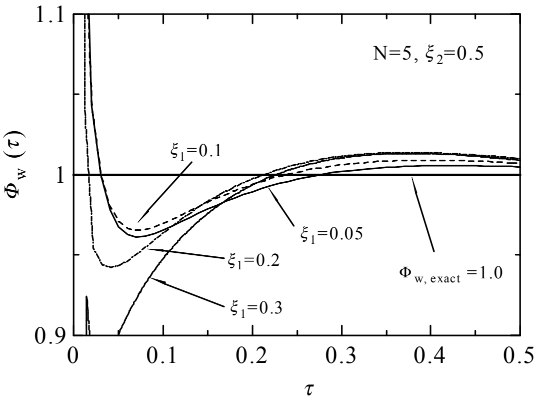

Fig. 5 Effect of measuring point on accuracy of solution (Case 3, Heat flux)

Order of approximate equation of Eq. (12)

It is found from Tables 2 and 3 that it is not expected any more even if increasing N to improve the accuracy of prediction and to reduce the minimum predictive time. Consequently, either value of N = 5 or 6 is recommended as the critical value.

Effect of Temperature Change on Estimation

The approximate equation for the surface temperature that its first derivative with respect to time becomes discontinues gives worse estimate than that for the surface temperature that its derivative is continues (See Monde, 2000 and Monde et al., 2000). In other words, for a smooth surface temperature change, the high accurate estimation can be reached.

TWO-DIMENSIONAL INVERSE HEAT CONDUCTION PROBLEM

For an isotropy rectangular system, two- dimensional heat conduction equation can be written in a non-dimensional form as:

$$\frac{\partial \theta}{\partial \tau} = \frac{\partial^2 \theta}{\partial \xi^2} + L^2 \frac{\partial^2 \theta}{\partial \eta^2} \qquad 0 < \xi < 1, \quad 0 < \eta < 1 \qquad (27)$$

General Solution for Two-dimensional Unsteady Heat Conduction

Assuming a uniform initial temperature (θ = 0) and applying Laplace transform to Eq. (27), we can easily reform Eq.(27) into Eq.(28) in a subsidiary form as:

$$\frac{\partial^2 \bar{\theta}}{\partial \xi^2} + L^2 \frac{\partial^2 \bar{\theta}}{\partial \eta^2} - s\bar{\theta} = 0 \qquad (28)$$

A general subsidiary solution becomes:

$$\bar{\theta}(\xi,\eta,s) = \{A\cos(m\xi) + B\sin(m\xi)\}\{C\cos(n\eta/L) + D\sin(n\eta/L)\} \qquad (29)$$

where m and n are undetermined constants and possess a relation confined by $m^2 + n^2 = -s$. The constants of A, B, C and D are integral constants subjected to surface condition. The four unknown constants here need four individual boundary conditions for four surfaces to close the equation. To simplify the question, we here consider two simplest cases only.

Insulation on Three Surfaces

As one of the simplest boundary conditions, three surfaces are insulated as given by the following equations and only one surface is left unknown, which corresponds to the IHTP solution.

$$\frac{\partial \bar{\theta}}{\partial \xi} = 0, \xi = 0,1$$

(30-a)

$$\frac{\partial \bar{\theta}}{\partial \eta} = 0, \eta = 1$$

(30-b)

A general solution that satisfies Eq. (30) becomes as:

$$\bar{\theta}(\xi,\eta,s) = \sum_{j=0}^{\infty} B_j \cos(m_j\xi)\cos\left\{\frac{n_j}{L}(1-\eta)\right\} \qquad (31)$$

where m_j (= $j\pi$) is eigenvalue to satisfy Eq. (30-a) and $\cos(m_j\xi)$ is the corresponding eigenfunction. The unknown constant B_j is going to be determined by using the temperature distribution measured on one plane $\eta = \eta_1$ inside the solid.

Insulations on Two Surfaces

If we assume that the surfaces at ξ = 0, 1 are insulated and that the boundary conditions on surfaces η = 0, 1 are unknown, that is, the known surface conditions:

$$\frac{\partial \bar{\theta}}{\partial \xi} = 0, \xi = 0,1$$

(32)

then general solution of Eq.(29) turns to:

$$\bar{\theta}(\xi,\eta,s) = \sum_{j=0}^{\infty} \cos(m_j\xi)\{A_j \sin(n\eta/L) + B_j \cos(n\eta/L)\} \qquad (33)$$

where m_j (= $j\pi$) and cos ($m_j\xi$) are still the same eigenvalue and eigenfunction, respectively, since the same boundary conditions on ξ = 0, 1 are set for Eq. (29) to be satisfied. The two unknown constants A_j and B_j are going to be determined by the measured temperatures on two different planes ($\eta = \eta_n$, n = 1, 2, $\eta_1 < \eta_2$) inside the solid.

Approximate Equation Depicting Temperature Variation on A Plane of $\eta = \eta_n$ (n = 1, 2) Inside The Solid

Temperature variations with time along coordinate ξ on a plane of $\eta = \eta_n$ (n = 1, 2) may be approximated from Eq. (34), in which the temperature variation with time is expressed by a half polynomial series.

$$f(\xi,\eta_n,\tau) = g(\xi)\sum_{k=0}^{N} \frac{b_k}{\Gamma(k/2+1)}(\tau - \tau_n^*)^{k/2} \quad n = 1,2 \qquad (34)$$

There are two reasons allowing us to adopt the form of half polynomial series of time here: (1) the general solution of heat conduction possesses the item of root of time; (2) one dimensional IHTP, which used the form of half polynomial series of time in temperature approximation, has achieved great success. In Eq. (34), a time lag, τ_n*, is determined by erfc(η_n /2√τ_n*) = min(θ), where min(θ) is a minimum readable division of temperature-measuring instrument.

Expanding $g(\xi)$ in Fourier series by using eigenfunction, $\cos(m_j\xi)$, we can get the following equation:

$$f(\xi,\eta_n,\tau)=\sum_{j=0}^{\infty}C_j\cos(m_j\xi)\sum_{k=1}^{N}\frac{b_k}{\Gamma(k/2+1)}(\tau-\tau_n^*)^{k/2} \quad (35)$$

As the most natural thought, one may expect the coefficients in Eq. (35), i.e., C_j and b_k, being solved separately by using, for example, the least mean square method. Unfortunately, the determined approximation function turns to be two-dimensional regression planes of ξ and τ and separate determination of C_j and b_k is impossible. To solve the problem, here we introduce coefficient $D_{j,k}$ to substitute C_j and b_k. Eq. (35) then is reformed to:

$$f(\xi,\eta_n,\tau)=\sum_{j=0}^{\infty}\cos(m_j\xi)\sum_{k=0}^{N}\frac{D_{j,k}}{\Gamma(k/2+1)}(\tau-\tau_n*)^{k/2} \quad (36)$$

Applying Eq. (36) to the temperatures measured at the points on $\eta=\eta_n$ (n = 1, 2), we can have the coefficient $D_{j,k}$ determined. Then performing Laplace transformation to Eq. (36), we can get in a subsidiary form as:

$$\bar{f}(\xi,\eta_n,s)=e^{-s\tau_n*}\sum_{j=0}^{\infty}\cos(m_j\xi)\sum_{k=0}^{N}D^{(n)}{}_{j,k}/s^{(k/2+1)} \quad n = 1, 2$$

(37)

Characteristics of Approximation Equation

Equation (36), which is used to approximate the temperatures measured on the plane of $\eta=\eta_n$, is determined by using Fourier series composed of eigenfunction of $\cos(j\pi\xi)$. As a characteristic of Fourier series, the increase of the employed eigenvalue generally improves its approximation. As a result, a requirement of a higher order of eigenvalue leads to an increase of the measuring points, which may allow us to encounter another difficulty in actual measurement and a complicate procedure in determining the coefficients of $D^{(n)}{}_{j,k}$. In addition to these, from the viewpoint of measurement with a thermocouple, the measured temperature always includes some uncertainty, for example, uncertainties of a level from 0.1 to 1 %. Therefore, the number of eigenvalue, N_j, would be restricted to a limited value, which will be discussed later.

Apart from the number of eigenvalue N_j, it is necessary to discuss the number of terms related to time. Monde (2000) recently reported that for the case of one-dimensional IHTP, the number of N, which is order of half polynomial series of time used in approximating temperature change, is recommended to range from 5 to 8, beyond which no improvement is expected.

Calculation of Surface Temperature

Applying Eq. (31) or Eq. (33) to $\eta=\eta_n$ (n = 1 or 2) and setting them equal to Eq. (37), we can have the coefficients of B_j in Eq. (31) or A_j and B_j in Eq. (33) determined, depending on the number of the unknown surface. After some manipulations, we can finally express the solution for the temperature change in the solid (including surfaces) in subsidiary forms as:

for boundary condition that three surfaces are insulated

$$\bar{\theta}(\xi,\eta,s)=e^{-s\tau_1^*}\sum_{j=0}^{N_j}\frac{\cos(m_j\xi)\cos\{\frac{n}{L}(1-\eta)\}}{\cos\{\frac{n}{L}(1-\eta_1)\}}\sum_{k=0}^{N}D_{j,k}^{(1)}/s^{(k/2+1)} \quad (38)$$

for boundary condition that two opposite surfaces are insulated

$$\bar{\theta}(\xi,\eta,s)=\frac{e^{-s\tau_1^*}\sum_{j=0}^{N_j}\sum_{k=0}^{N}\frac{D_{j,k}^{(1)}}{s^{(k/2+1)}}\cdot\sin\{(n/L)(\eta_2-\eta)\}}{\sin\{(n/L)(\eta_2-\eta_1)\}}\cos(m_j\xi)-\frac{e^{-s\tau_2^*}\sum_{j=0}^{N_j}\sum_{k=0}^{N}\frac{D_{j,k}^{(2)}}{s^{(k/2+1)}}\cdot\sin\{(n/L)(\eta_1-\eta)\}}{\sin\{(n/L)(\eta_2-\eta_1)\}}\cos(m_j\xi) \quad (39)$$

Substitution of $n = i\sqrt{(s+m_j^2)}$ into $\cos(n/L)$ and $\sin\{n/L(\eta_2-\eta)\}$ reforms them into $\cosh\{\sqrt{(s+m_j^2)}/L\}$ and $i\sinh\{\sqrt{(s+m_j^2)}/L\}$, respectively. Taking account into these relations and setting $\eta = 0$ in Eq. (39), we can obtain the surface temperature as:

for boundary condition that three surfaces are insulated

$$\bar{\theta}_w(\xi,s)=e^{-s\tau_1^*}\sum_{j=0}^{N_j}\frac{\cos(m_j\xi)\cosh(\sqrt{s+m_j^2}/L)}{\cosh\{(\sqrt{s+m_j^2}/L)(1-\eta_1)\}}\sum_{k=0}^{N}D_{j,k}^{(1)}/s^{(k/2+1)} \quad (40)$$

for boundary condition that two opposite surfaces are insulated

$$\bar{\theta}_w(\xi,s)=e^{-s\tau_1^*}\sum_{j=0}^{N_j}\frac{\sinh\{(\sqrt{s+m_j^2}/L)\eta_2\}\cos(m_j\xi)}{\sinh\{(\sqrt{s+m_j^2}/L)(\eta_2-\eta_1)\}}\sum_{k=0}^{N}\frac{D_{j,k}^{(1)}}{s^{(k/2+1)}}-e^{-s\tau_2^*}\sum_{j=0}^{N_j}\frac{\sinh\{(\sqrt{s+m_j^2}/L)\eta_1\}\cos(m_j\xi)}{\sinh\{(\sqrt{s+m_j^2}/L)(\eta_2-\eta_1)\}}\sum_{k=0}^{N}\frac{D_{j,k}^{(2)}}{s^{(k/2+1)}} \quad (41)$$

Expanding Hyperbolic functions in Eqs. (40) and (41) in series around $s = 0$ and then performing inverse Laplace transformation, we can get the surface temperatures for the two different kinds of boundary condition as:

for boundary condition that three surfaces are insulated

$$\theta_w(\xi,\tau)=\sum_{j=0}^{N_j}\sum_{k=-1}^{N}\frac{G_{j,k}^{(1)}\cos(m_j\xi)}{\Gamma(k/2+1)}(\tau-\tau_1^*)^{k/2} \quad (42)$$

for boundary condition that two opposite surfaces are insulated

$$\theta_w(\xi,\tau)=\sum_{j=0}^{N_j}\sum_{k=-1}^{N}\frac{G_{j,k}^{(1,2)}\cos(m_j\xi)}{\Gamma(k/2+1)}(\tau-\tau_1^*)^{k/2} -\sum_{j=0}^{N_j}\sum_{k=-1}^{N}\frac{G_{j,k}^{(2,1)}\cos(m_j\xi)}{\Gamma(k/2+1)}(\tau-\tau_2^*)^{k/2} \quad (43)$$

Detailed procedure to calculate these coefficients in Eqs. (42) and (43) in noted in appendix.

Calculation of Surface Heat Flux

By differentiating Eqs. (38) and (39) with respect to η, the heat flux in η direction can be derived and then the surface heat flux is achieved by setting $\eta = 0$:

for boundary condition that three surfaces are insulated

$$\overline{\Phi}_w(\xi,s)=e^{-s\tau_1^*}\sum_{j=0}^{N_j}\frac{(\sqrt{s+m_j^2}/L)\sinh(\sqrt{s+m_j^2}/L)}{\cosh\{(\sqrt{s+m_j^2}/L)(1-\eta_1)\}} \times\sum_{k=0}^{N}D_{j,k}^{(1)}/s^{(k/2+1)}\cos(m_j\xi) \quad (44)$$

for boundary condition that two opposite surfaces are insulated

$$\overline{\Phi}_w(\xi,s)=e^{-s\tau_1^*}\sum_{j=0}^{N_j}\frac{(\sqrt{s+m_j^2}/L)\cosh\{(\sqrt{s+m_j^2}/L)\eta_2\}}{\sinh\{(\sqrt{s+m_j^2}/L)(\eta_2-\eta_1)\}} \times\sum_{k=0}^{N}\frac{D_{j,k}^{(1)}}{s^{(k/2+1)}}\cos(m_j\xi) -e^{-s\tau_2^*}\sum_{j=0}^{N_j}\frac{(\sqrt{s+m_j^2}/L)\cosh\{(\sqrt{s+m_j^2}/L)\eta_1\}}{\sin\{(\sqrt{s+m_j^2}/L)(\eta_2-\eta_1)\}} \times\sum_{k=0}^{N}\frac{D_{j,k}^{(2)}}{s^{(k/2+1)}}\cos(m_j\xi) \quad (45)$$

Just as the same as what we did in deriving the surface temperature, in achieving the surface heat flux, we also need to expand Hyperbolic functions in Eqs. (44) and (45) in series around $s = 0$ and perform inverse Laplace transform. The surface fluxes for the two different kinds of boundary condition are finally expressed as:

for boundary condition that three surfaces are insulated

$$\Phi_w(\xi,\tau)=\sum_{j=0}^{N_j}\sum_{k=-1}^{N}\frac{H_{j,k}^{(1)}\cos(m_j\xi)}{\Gamma(k/2+1)}(\tau-\tau_1^*)^{k/2} \quad (46)$$

for boundary condition that two opposite surfaces are insulated

$$\Phi_w(\xi,\tau)=\sum_{j=0}^{N_j}\sum_{k=-1}^{N}\frac{H_{j,k}^{(1,2)}\cos(m_j\xi)}{\Gamma(k/2+1)}(\tau-\tau_1^*)^{k/2} -\sum_{j=0}^{N_j}\sum_{k=-1}^{N}\frac{H_{j,k}^{(2,1)}\cos(m_j\xi)}{\Gamma(k/2+1)}(\tau-\tau_2^*)^{k/2} \quad (47)$$

Detailed process to derive the coefficient in Eqs. (46) and (47) is found is Appendix III.

Discussion on Approximate Equation for Temperature Variation

Using Eqs. (40) and (41) and Eqs. (46) and (47), we can predict the surface temperature and heat flux explicitly. However, just as the same as what we discussed in one-dimensional IHTP (Monde, 2000), when the Laplace operator s is high enough, Eq. (37) has a characteristic of becoming divergence. As concerned with the inverse Laplace transformation, there exists a minimum time, only after which the inverse solutions (Eqs. (42) and (43) for surface temperature and Eqs.(46) and (47) for surface heat flux) become applicable. In another word, it is possible for the inverse solution near $s = 0$ to predict the surface temperature and heat flux after the minimum time τ_{min}.

SIMPLE EXAMPLES FOR VERIFICATION OF THE PRESENT METHOD

In order to verify the applicability of Eqs. (42) and (43) and Eqs. (46) and (47), we need the temperatures measured on a plane of $\eta = \eta_n$ (n = 1, 2). Here, the temperatures calculated from a direct solution, which is derived for a given boundary condition mentioned below, are used as the measured temperatures. If the boundary conditions are that the surfaces on $\xi = 0$, 1 or even on $\eta = 1$ are insulated as given by Eq. (32) or Eq. (30) and the left surface of $\eta = 0$ is given by either Eq. (48-a) or (48-b), which will correspond to the IHTP solution,

(6) $\theta = 1$, $0 < \xi < 0.5$, $\theta = 0$, $0.5 < \xi < 1.0$, $\eta = 0$ (48-a)

(7) $\Phi = 1$, $0 < \xi < 0.5$, $\Phi = 0$, $0.5 < \xi < 1.0$, $\eta = 0$

(48-b)

then, direct solutions for the surface condition of cases (6) and (7) on $\eta = 0$ can be obtained, respectively.

The exact value of the temperatures on any plane of $\eta = \eta_n$ (n = 1, 2) are easily calculated from the direct solution. As actual temperatures measured on $\eta = \eta_n$ always include some uncertainty, we may superpose normal random error on the exact value of the temperature as given by the following equation similar to the one-dimensional case:

$$\theta(\xi,\eta_n,\tau)=\theta_{exact}(\xi,\eta_n,\tau)(1+0.5\cdot10^{-N_{sf}}\varepsilon) \quad (49)$$

and then we determine the coefficients of $D^{(n)}_{j,k}$ in Eq. (36) using the temperature given by Eq. (49) in which N_{sf} is the order of significant figure and ε is normal random error having average value of $m = 0$ and standard deviation of $\sigma = 1$.

Figure 6 shows the variation of temperatures on $\eta = 0.01$ calculated from Eq. (49), for example, for the boundary condition (case 6) given by Eq. (48-b). These temperatures on η = 0.01 are used to determine the coefficients of $D^{(n)}_{j,k}$ in Eq. (36). Figure 7 shows the temperatures approximated by Eq. (36), in which the determined coefficients of $D^{(n)}_{j,k}$ is used.

NUMERICAL CALCULATION RESULTS AND DISCUSSIONS

Figures 8 and 9 show the surface temperature estimated by Eq. (43) and the surface heat flux estimated by Eq. (47) for the case (7). Figure 10 shows the surface temperature estimated by Eq. (42) for the case (6). The temperatures used in the calculations are on two planes of η_1 = 0.01 and η_2 = 0.05 and the measuring points on each plane are set at 30. In addition, orders of N_j and N in Eq. (36) are set at 30 and 5, respectively. The order of significant figures is set at N_{sf} = 3, which can be considered an enough error level that is included in a measurement of temperature with a thermocouple.

Figure 11 shows the surface heat flux for the case (7) estimated by Eq. (46) by using the temperatures only on one plane of η_1 = 0.01. The orders of N_j, N and N_{sf} are kept as the same as that used in the previous calculation, that is, N_j = 30, N = 5 and N_{sf} = 3.

It may be necessary to mention that for the case (6), the temperature on the surface possesses a discontinuity point at ξ = 0.5 so that the surface heat flux obtained by differentiating the temperature with respect to η does not converge uniformly at ξ = 0.5. Consequently, the predicted surface heat flux at ξ = 0.5 is, of course, divergent. Under such circumstance, as shown in Fig. 10, only the prediction to the surface temperature is possible from the inverse solution.

Finally, it may be worth mentioning that although the surface temperature for the case (7) predicted from Eq. (42), which is not illustrated here, is a little inferior to that predicted from Eq. (43), it is much better than the predicted surface heat flux as shown in Fig. 11.

It is concluded from a comparison of Figs. 9, 10, and 11 that the inverse solutions obtained from two measuring planes can estimate the surface temperature as well as the surface heat flux at much higher accuracy than those obtained from only one measuring plane. How the relative positions of the two planes (η = η_n) affect on the predictive accuracy would be expected as one of the future researches.

Discussion to the Prediction Result

Figure 9 shows that the surface temperature estimated by Eq. (47) approaches to the given surface temperature and agrees it with an error of a few percent after a time whose Fourier number becomes 0.02. As for the surface temperature estimated by Eq. (43), it is found from Fig. 10 that the whole surface

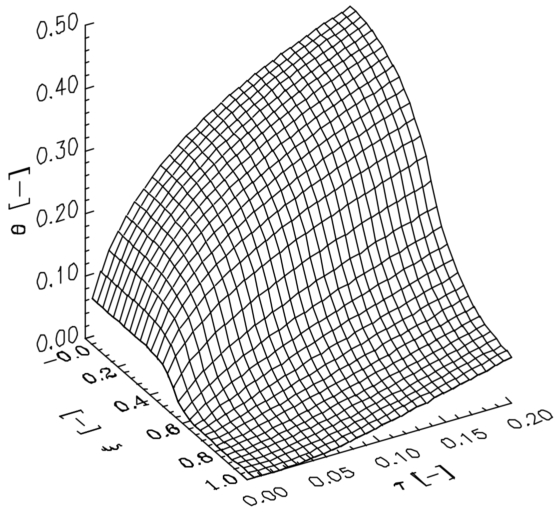

Fig. 6 Temperature change in a solid at η_1 = 0.01 calculated from Eq. (49) for the case (7)

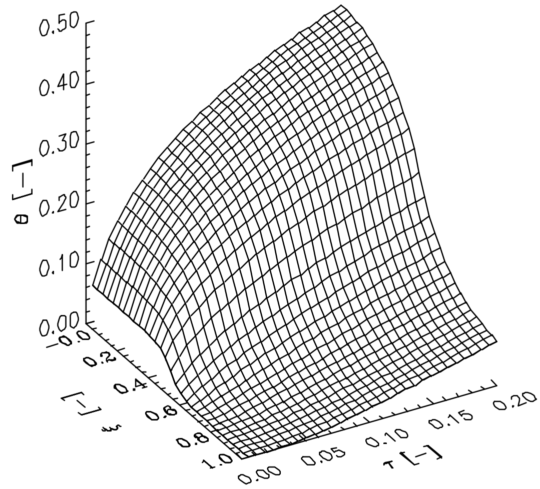

Fig. 7 Temperature approximated by using Eq. (36) at η_1 = 0.01 for the case (7)

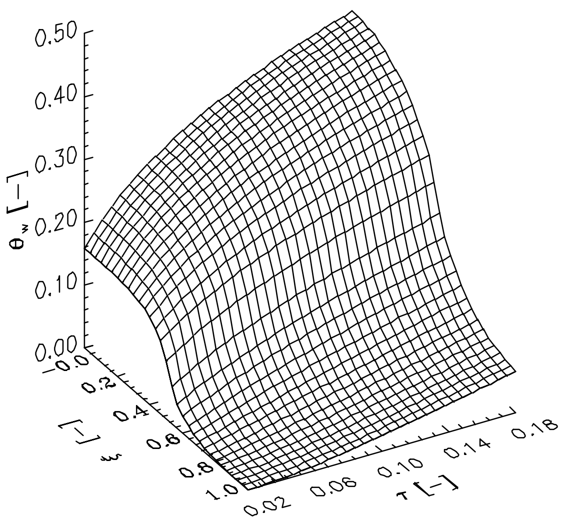

Fig. 8 Surface temperature estimated by Eq. (43) for the case (7)

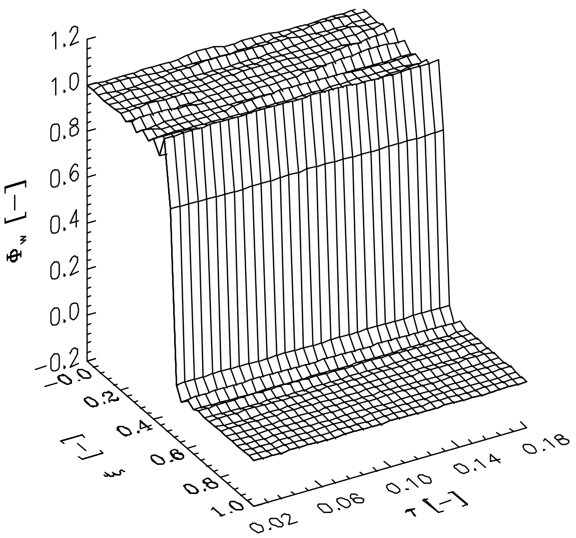

Fig. 9 Surface heat flux estimated by Eq. (47) for the case (7)

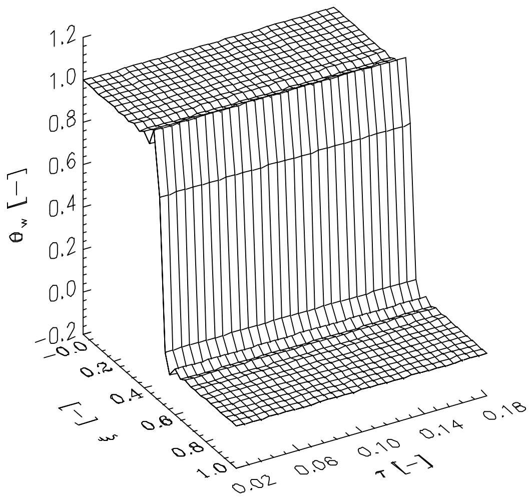

Fig. 10 Surface temperature estimated by Eq. (43) for the case (6)

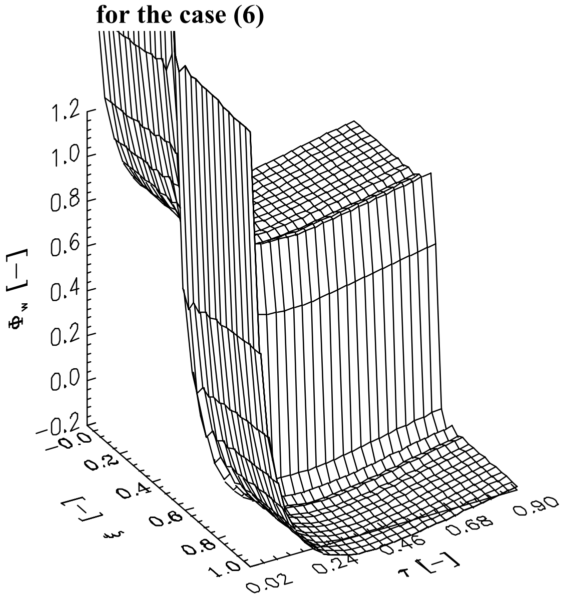

Fig. 11 Surface heat flux estimated by Eq. (46) for the case (7)

temperatures are well predicted inside an error band of 1%, although the estimated surface temperature seems slightly deviating from the given temperature near the discontinuity point of $\xi = 0.5$. Whereas for the case (7), because there exists no discontinuity of the temperature at any point on the surface as what we may have already observed from Fig. 8, the inverse solution, Eq. (43), predicts the surface temperature very well within an error band of 1%. However, the existence of the discontinuity point for the surface heat flux at $\xi = 0.5$ makes accuracy of its prediction degrade obviously and the estimated values present an error near to 10% around $\xi = 0.5$, as shown in Fig. 9. The whole prediction, however, despite of the existence of the discontinuity point, is still found of satisfactory accuracy.

To the cases (6) and (7) listed above, the inverse solutions of Eqs. (43) and (47) are found being capable of predicting the surface temperature and heat flux in an error band from 3 to 5%. As a general, from doing comparison to Figs. 9 and 10, we can find that the prediction to the surface temperature is better than that to the surface heat flux. The reason is analyzed due to the temperature disturbance included in Eq. (49) being enlarged in the calculation of the heat flux, where the temperature difference is needed between the measuring points.

Influence of Discontinuity Point

As shown in Figs. 9 and 10, a degradation of prediction accuracy is observed near the discontinuity point. The reason is attributed to the employment of the Fourier series in the temperature approximation Eq. (36). In other words, the Gibbs phenomenon, which is a characteristic phenomenon in the Fourier series, is aroused near the discontinuity point of $\xi = 0.5$. From engineering point of view, a problem of discontinuity generally doesn't exist because usual boundary condition always possesses no discontinuity point. In another word, for actual engineering condition that possesses no discontinuity point on boundary, the proposed IHTP solution can be anticipated for high prediction accuracy.

Influence of Degree of Eigenvalue Employed in Eq. (36)

The improvement of the temperature approximation accuracy in Eq. (36) is considered being the most important and effective way to improve the accuracy of the whole IHTP solution. As a most natural consideration, the increase of the number of eigenvalue

N_j may lead to the improvement of temperature approximation accuracy and consequently the improvement of the accuracy of the whole IHTP solution. To check a possible influence of the number of eigenvalue N_j, we increase the number to 40. However, no obvious improvement of the accuracy that is expected accordingly is observed. The reason is attributed to the uncertainties included in the measured temperatures, from which the coefficients in Eqs. (36) and (37) are determined. In another word, accuracy improvement from the increasing of the number of eigenvalue may be counteracted by the uncertainties included in the measured temperatures. Therefore, in spite of any increase in the number of eigenvalue, the approximation accuracy cannot be improved significantly. The influence of N_j on the accuracy

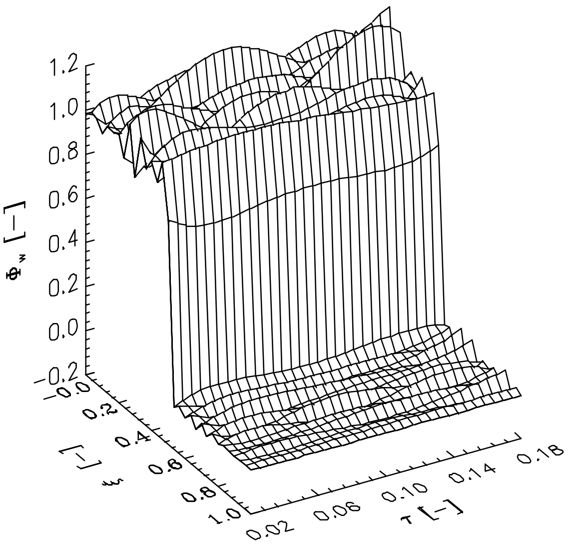

Fig. 12 Surface heat flux estimated by Eq. (47) for the case (7) with an error of N_{sf} = 2

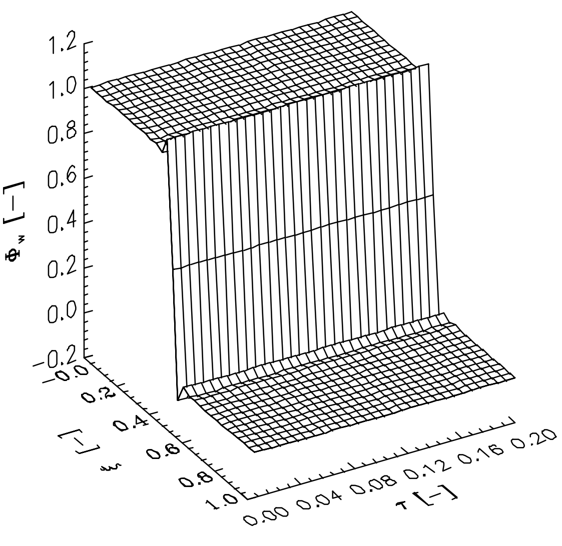

Fig. 13 Surface heat flux estimated for the case (7) without error by Eq. (47)

therefore associates to the error included in the measured data greatly. In the future, the accuracy improvement due to the increase of N_j needs to be examined by concerning the accuracy of the measured temperature.

Influence of the Temperature Measurement Accuracy

To check the influence of the accuracy of the measured temperature over prediction result, we set the order of significant figure N_{sf} in Eq. (49) at 2, 3 and ∞ (error-free). Corresponding results are shown in Figs. 12 and 13, respectively.

When N_{sf} is 2, as shown in Fig. 10, the prediction result is much poor than that when N_{sf} is set at 3. The predicting error is about 20%. And the IHTP solution calculated from error-free temperature, as shown in Fig. 13, still possesses an error about 4%, which is almost as the same as that calculated from N_{sf} = 3. The influencing tendency tells us an importance of the measured data at high accuracy. In actual measurement, although the measured temperature definitely includes some uncertainty, an effort of employing high precision instrument may lead directly to an improvement of predicting accuracy for the IHTP solution.

CONCLUSIONS

By using the Laplace transformation technique, we achieved two-dimensional IHTP solutions and following results:

1. Surface temperature can be predicted well over the whole surface within an error of a few percent, if it changes continuously.
2. The minimum predictive time for the proposed IHTP solution is τ = 0.02.
3. In order to predict the surface temperature and heat flux from the proposed IHTP solution successfully, a high precision instrument that can ensure measured temperature at uncertainty level less than 0.1 %, namely N_{sf} = 3 at least, is recommended.

REFERENCES

Alifanov, O. M., "*Inverse Heat Transfer Problems*", Springer-Verlag, pp. 5 - 8, (1994).

Arima, H., Monde, M. and Mitsutake, Y., 2001, "Estimation of Surface Temperature and Heat Flux using Inverse Solution for One Dimensional Heat Conduction" (in Japanese), *Thermal Science & Engineering*, 9 – 2, pp. 9 – 20, (2001).

Beck, J. V., "*Inverse Heat Conduction*", (1985), A Wiley-Interscience Publication.

Bell, G. E., "An Inverse Solution for the Steady Temperature Field within a Solidified Layer", *Int. J. of Heat and Mass Transfer,* 27 - 12, pp. 2331 - 2337, (1984).

Burggraf, O. R., "An Exact Solution of the Inverse Problem in Heat Conduction Theory and Application", *J. Heat Transfer*, 86, pp. 373 - 382, (1964).

Frankel, J. I., "A Global Time Treatment for Inverse Heat Conduction Problems", *J. Heat Transfer*, 119 - 4, 673 - 683, (1997).

Hsieh, C. K. and Su, K. C., "A Methodology of Predicting Cavity Geometry Based on Scanned Surface Temperature Data – Prescribed Surface Temperature at the Cavity Side", *J. Heat Transfer*, 102 - 2, pp. 324 - 329, (1980).

Huang, C. H. and Tsai, C. C., "An inverse heat conduction problem of estimating boundary fluxes in an irregular domain with conjugate gradient method", *Heat and Mass Transfer*, 34, pp. 47-54, (1998).

Imber, M. and Khan J., "Prediction of Transient Temperature Distributions with Embedded Thermo-couples", *AIAA Journal*, 10 - 6, pp. 784 - 789, (1972).

Imber, M., "Temperature Extrapolation Mechanism for Two-Dimensional Heat Flow", AIAA Journal, 12 - 8, pp. 1089 - 1093, (1974).

Lithouhi, B. and Beck, J. V., "Multinode Unsteady Surface Element Method with Application to Contact Conductance Problem", *J. Heat Transfer*, 108 - 2, pp. 257 - 263, (1986).

Monde, M., "Analytical method in inverse heat transfer problem using Laplace transform technique", *Int. J. of Heat and Mass Transfer*, 43, pp. 3965 - 3975, (2000)

Monde, M., Arima, H. and Mitsutake, Y., "Analytical Method In Inverse Heat Transfer Problem Using Laplace Transform Technique - Second And Third Boundary Conditions -", 3rd European thermal Science Conference 2000, Sept. 10 - 13, 2000, (Heidelberg).

Monde, M., and Mitsutake, Y., "A New Estimation Method of Thermal Diffusivity Using Analytical Inverse Solution for One Dimensional Heat Conduction", *Int. J. of Heat and Mass Transfer*, 44 - 16, pp. 3169 – 3177, (2001).

Monde, M., Arima, H., Liu, W., Mitsutake, Y., and Mammod, J., "Analytical Solution for Two-Dimensional Inverse Heat Conduction Problem using Laplace Transformation", (Submitted in J. Heat Transfer).

Shoji, M. and Ono, N., "Application of the boundary element to the inverse problem of heat conduction (in Japanese)", *Trans. JSME*, Ser. B, 54 - 506, pp. 2893 - 2900, (1988).

Shoji, M., "Study of inverse problem of heat conduction (in Japanese)", *Trans. JSME*, 44-381, pp. 1633 - 1643, (1978).

NOMENCLATURE

$A_{j,n}$	:coefficient	
a	:thermal diffusivity	[m^2/s]
a_0, a_1, a_2	:coefficient of initial temperature distribution	
B_j	:coefficient	
b_k	:coefficient	
$D_{j,k}$	:coefficient derived from measured temperature variation	
$f_1(\tau)$, $f_2(\tau)$	:function of non-dimensional temperature at a point of ξ_1, ξ_2	
$f(\xi, \eta_n, \tau)$	:function for approximating temperatures on plane $\eta = \eta_n$ inside a solid	
L	:aspect ratio ($=L_x/L_y$)	
L_x	:length of a solid in x direction	
L_y	:length of a solid in y direction	
m	:average for a value of ε	
min(θ)	:minimum of significant number or minimum division of measuring equipment	
m_j	:eigenvalue ($m_j = j\pi$)	
N	:degree of approximate polynomial with time	
N_j	:degree of eigenvalue	
N_{sf}	:order of significant figure	
n	:constant ($= i\sqrt{s+m^2}$)	
p	:= $\sqrt{s}$	
q	:heat flux	[W/m^2]
q_o	:heat generated per volume unit	[W/m^3]
R	:characteristic length on the cylindrical and spherical coordinate	[m]
s	:Laplace operator ($= p^2$ or $= -(m^2 + n^2)$)	
T	:temperature	[K]
T_0	:characteristic temperature	[K]
t	:time	[s]
x, y	:x and y coordinates, respectively	[m]
W_r, W_c, W_s	:influence functions of initial temperature for rectangular, cylindrical and spherical coordinate	
Y_r, Y_c, Y_s	:influence functions of initial temperature for rectangular, cylindrical and spherical coordinate	
ε	:random error varying from –1 to 1	
Φ	:non-dimensional heat flux	
$\overline{\Phi}$	:subsidiary value of Φ	

$\Gamma(n)$	:gamma function
θ	:Non-dimensional temperature
$\bar{\theta}$	:subsidiary value of θ
θ_o	:initial temperature (distribution)
τ	:non-dimensional time (Fourier number = at/L^2 , at/R^2 or at/L_x^2)
τ_1	:minimum predictive time
τ_1^*	:non-dimensional time lag ($erfc(\xi_i / 2\sqrt{\tau_i^*}) = \min(\theta)$)
ξ	:non-dimensional length ($= x/L$, r/R, $\xi_1 < \xi_2$ or x/L_x)
η	:non-dimensional distance in y direction ($= y/L_y$), $\eta_1 < \eta_2$)
σ	:standard deviation

Subscript

1,2	: Measuring temperature
c	: Cylindrical coordinate
r	: Rectangular coordinate
s	: Spherical coordinate
w	: Surface

Appendix I

Functions for initial temperature distributions

$$F_1(a_0, a_2, s) = \frac{a_0}{s} + \frac{2a_2}{s^2}$$

$$G_1(a_1, s) = -\frac{a_1}{s}$$

$$F_2(a_0, a_2, s) = \frac{a_0}{s} + \frac{a_2}{s} + \frac{4a_2}{s^2}$$

$$G_2(a_1, a_2, s) = -\frac{a_1}{s} - \frac{2a_2}{s}$$

$$F_3(a_0, a_1, a_2, s) = \frac{a_0}{s} + \frac{a_1}{s} + \frac{a_2}{s} + \frac{6a_2}{s^2}$$

$$G_3(a_1, a_2, s) = \frac{a_1}{s} - \frac{2a_2}{s}$$

$$W_r = -2a_2(c_{1,2} - c_{1,1}) - a_2(c_{0,2}\xi_1^{\ 2} - c_{0,1}\xi_2^{\ 2})$$

$$Y_r = -2a_2(d_{1,2} - d_{1,1}) - a_2(d_{0,2}\xi_1^{\ 2} - d_{0,1}\xi_2^{\ 2})$$

$$W_c = -4a_2(c_{1,2} - c_{1,1}) - a_2(c_{0,2}\xi_1^{\ 2} - c_{0,1}\xi_2^{\ 2}) + a_2$$

$$Y_c = -4a_2(d_{1,2} - d_{1,1}) - a_2(d_{0,2}\xi_1^{\ 2} - d_{0,1}\xi_2^{\ 2}) - 2a_2$$

$$W_s = -6a_2(c_{1,2}\xi_1 - c_{1,1}\xi_2) - a_2(c_{0,2}\xi_1^{\ 3} - c_{0,1}\xi_2^{\ 3}) + a_2$$

$$Y_s = -6a_2(d_{1,2}\xi_1 - d_{1,1}\xi_2) - a_2(d_{0,2}\xi_1^{\ 3} - d_{0,1}\xi_2^{\ 3}) - 2a_2$$

Appendix II.

Expansion equation for one-dimensional IHTP

The subsidiary form obtained after executing the Laplace transformation function can be abbreviated into $\bar{\theta} = \bar{f}(s)K(s)$. The inverse Laplace transformation of this subsidiary function becomes as:

$$\theta(\tau) = \frac{1}{2\pi i}\int_{c-i\infty}^{c+i\infty} e^{s\tau}\bar{\theta}(s)ds$$

In the present analysis, we first expand the functions K(s) around s = 0 in a series, and then obtained the solution by executing complex integration. The subsidiary functions of the surface temperature and heat flux expressed the kernel K(s).

(a) Finite body

Surface temperature:

$$\bar{\theta} = \bar{f}_1(s)K_{1,2}(s) - \bar{f}_2(s)K_{1,1}(s) - (\theta_0(\xi_1)/s + A_1/s^2)K_{1,2}(s)$$
$$+ (\theta_0(\xi_2)/s + A_2/s^2)K_{1,1}(s) + F(s)$$

Surface heat flux:

$$\bar{\Phi} = \bar{f}_1(s)K_{2,2}(s) - \bar{f}_2(s)K_{2,1}(s) - (\theta_0(\xi_1)/s + A_1/s^2)K_{2,2}(s)$$
$$+ (\theta_0(\xi_2)/s + A_2/s^2)K_{2,1}(s) + G(s)$$

where, A_1=A_2= $2a_2$ corresponds to rectangular, A_1=A_2= $4a_2$ to cylindrical one, A_1= $6a_2\xi_1$, A_2= $6a_2\xi_2$ to spherical one

(b) Semi-infinite body

Surface Temperature: $\bar{\theta} = \bar{f}_1(s)K_3(s)$

Surface heat flux : $\bar{\Phi} = \bar{f}_1(s)K_4(s)$

where, functions of F (s) and G (s) are related to initial temperature distribution (See appendix I).

(1) Expansion equation for finite body

Expansions of the kernel $K_{1,n}$(s), $K_{2,n}$(s) (n=1, 2) around s = 0 in a series for several coordinates are given as:

$$K_{1,n}(s) = \sum_{j=0}^{\infty} c_{j,n}s^j \qquad n = 1, 2$$

$$K_{2,n}(s) = \sum_{j=0}^{\infty} d_{j,n}s^j \qquad n = 1, 2$$

The coefficients $c_{j,n}$ and $d_{j,n}$ can be given as:

$$c_{j,n} = \frac{1}{g_0}\sum_{i=0}^{j} x_{i,n}h_{j-i} \qquad n = 1,2$$

$$d_{j,n} = \frac{1}{g_0}\sum_{i=0}^{j} y_{i,n}h_{j-i} \qquad n = 1,2$$

where, the coefficients $x_{i,,n}$ and $y_{i,n}$ are defined in Table A1 (a) to (c), and function h_j is also defined by the following equations, where g_i is shown in Table A1.

$$h_0 = 1$$
$$h_1 = -g_1$$
$$h_2 = -g_2 + g_1^{\ 2}$$
$$h_3 = -g_3 + 2g_1g_2 - g_1^{\ 3}$$

$$h_4 = -g_4 + (2g_1g_3 + g_2^{\ 2}) - 3g_1^{\ 2}g_2 + g_1^{\ 4}$$

[illegible]

We can express the surface temperature $\overline{\theta_w}(s)$ and heat flux $\overline{\Phi}_w(s)$ using these coefficients in a subsidiary form as

$$\bar{\theta}_w = e^{-s\tau_1^*}\sum_{i=0}^{N}\frac{b_{i1}}{s^{i/2+1}}\sum_{j=0}^{\infty}c_{j,2}s^j - e^{-s\tau_2^*}\sum_{i=0}^{N}\frac{b_{i2}}{s^{i/2+1}}\sum_{j=0}^{\infty}c_{j,1}s^j$$

$$= e^{-s\tau_1^*}\sum_{j=-1}^{N}\frac{C_{j,12}}{s^{j/2+1}} - e^{-s\tau_2^*}\sum_{j=-1}^{N}\frac{C_{j,21}}{s^{j/2+1}}$$

where

$$C_{-1,lm} = \sum_{k=0}^{Nk} b_{2k+1,l}c_{k+1,m}, \quad Nk = \text{Int}\{(N-1)/2\} \quad l,m = 1,2 \text{ or } 2,1$$

$$C_{j,lm} = \sum_{k=0}^{Nk} b_{2k+j,l}c_{k,m}, \quad j \ge 0, Nk = \text{Int}\{(N-j)/2\} \quad l,m = 1,2 \text{ or } 2,1$$

$$\overline{\Phi}_w = e^{-s\tau_1^*}\sum_{j=-1}^{N}\frac{D_{j,12}}{s^{j/2+1}} - e^{-s\tau_2^*}\sum_{j=-1}^{N}\frac{D_{j,21}}{s^{j/2+1}}$$

where

$$D_{-1,lm} = \sum_{k=0}^{Nk} b_{2k+1,l}d_{k+1,m}, \; Nk = \text{Int}\{(N-1)/2\} \quad l,m = 1,2 \text{ or } 2,1$$

$$D_{j,lm} = \sum_{k=0}^{Nk} b_{2k+j,l}d_{k,m}, \; j \ge 0, Nk = \text{Int}\{(N-j)/2\} \quad l,m = 1,2 \text{ or } 2,1$$

The coefficients C_{ij}, and D_{ij} are the same coefficient of Eqs. (14) and (15).

(2) Expansion equation for the case of semi-infinite body

Expansions of the kernel K_1 (s), K_2 (s) around s = 0 in a series are given as:

$$K_1(s) = \sum_{i=0}^{\infty}u_i s^i, \quad K_2(s) = \sum_{i=0}^{\infty}v_i s^i$$

where, u_i and v_i are given in Table A2

We can express the surface temperature $\overline{\theta_w}(s)$ and heat flux $\overline{\Phi}_w(s)$ using these coefficients in a subsidiary form as:

$$\bar{\theta}_w = e^{-s\tau_1^*}\sum_{i=0}^{N}\frac{b_{i,1}}{s^{i/2+1}}\sum_{j=0}^{\infty}u_j s^j = e^{-s\tau_1^*}\sum_{j=-1}^{N}\frac{U_j}{s^{j/2+1}}$$

where

$$U_{-1} = \sum_{k=0}^{Nk} b_{k,1}u_{k+1}, \qquad Nk = N$$

$$U_j = \sum_{k=0}^{Nk} b_{k+j,1}u_k, \qquad j \ge 0, Nk = N-j$$

$$\overline{\Phi}_w = e^{-s\tau_1^*}\sum_{i=0}^{N}\frac{b_{i,1}}{s^{i/2+1}}\sum_{j=0}^{N}v_j s^j = e^{-s\tau_1^*}\sum_{j=-1}^{N}\frac{V_j}{s^{j/2+1}}$$

where

$$V_{-1} = \sum_{k=0}^{Nk} b_{k,1}v_k, \qquad Nk = N$$

$$V_j = \sum_{k=0}^{Nk} b_{k+j+1,1}v_k, \qquad j \ge 0, Nk = N-j-1$$

The coefficients U_j and V_j are the same coefficients of Eqs. (24) and (25).

Appendix III
Expansion equation for two-dimensional IHTP

(a) For the condition that insulations are done on three surfaces

Surface Temperature: $\bar{\theta} = \sum_{j=0}^{Nj}\bar{f}_1(s)K_{1,j}(s)$

Surface heat flux : $\bar{\Phi} = \sum_{j=0}^{Nj}\bar{f}_{1,j}(s)K_{2,j}(s)$

(b) For the condition that insulations are done on two opposite surfaces

Surface Temperature:

$$\bar{\theta} = \sum_{j=0}^{Nj}\left\{\bar{f}_1(s)K_{1,j}^{(2)}(s) - \bar{f}_2(s)K_{1,j}^{(1)}(s)\right\}$$

Surface heat flux:

$$\bar{\Phi} = \sum_{j=0}^{Nj}\left\{\bar{f}_{1,j}(s)K_{2,j}^{(2)}(s) - \bar{f}_{2,j}(s)K_{2,j}^{(1)}(s)\right\}$$

In spite of coordinate systems, kernels of $K_{1,j}^{(l)}(s)$ and $K_{2,j}^{(l)}(s)$ (l = 1, 2) expanded in a series around s = 0 are always written in a common form as:

$$K_{1,j}^{(l)}(s) = Co_{1,j}^{(l)}\sum_{n=0}^{\infty}c_{n,j}^{(l)}s^n \qquad l = 1, 2$$

$$K_{2,j}^{(l)}(s) = Co_{2,j}^{(l)}\sum_{n=0}^{\infty}d_{n,j}^{(l)}s^n \qquad l = 1, 2$$

The coefficients $c_{n,j}$ and $d_{n,j}$ are written as:

$$c_{n,j}^{(l)} = \frac{1}{g_0}\sum_{i=0}^{n}x_{i,j}^{(l)}h_{n-i} \qquad l = 1,2$$

$$d_{n,j}^{(l)} = \frac{1}{g_0}\sum_{i=0}^{n}y_{i,j}^{(l)}h_{n-i} \qquad l = 1,2$$

where h_j is calculated from following listed equations. The calculation to the employed item g_j and coefficients $x_{i,j}$, $y_{i,j}$ are listed in Table A3.

$$h_0 = 1$$
$$h_1 = -g_1$$
$$h_2 = -g_2 + g_1^2$$
$$h_3 = -g_3 + 2g_1g_2 - g_1^3$$

$$h_4 = -g_4 + (2g_1g_3 + g_2^2) - 3g_1^2g_2 + g_1^4$$
$$h_5 = -g_5 + 2(g_1g_4 + g_2g_3) - 3(g_1^2g_3 + g_1g_2^2) + 4g_1^3g_2 - g_1^5$$

With rearrangement, $\bar{\theta}_w(s)$ and $\bar{\Phi}_w(s)$ are derived as:

(1) For the condition that insulations are done on three surfaces

$$\bar{\theta}_w(s) = e^{-s\tau_1^*}\sum_{j=0}^{\infty}\sum_{k=0}^{N}\frac{D_{j,k}^{(1)}\cos(m_j\xi)}{s^{(k/2+1)}} * \sum_{n=0}^{\infty} Co_{1,j}^{(1)} c_{n,j}^{(1)} s^n$$
$$= e^{-s\tau_1^*}\sum_{j=0}^{\infty}\sum_{k=-1}^{N}\frac{G_{j,k}^{(1)}}{s^{(k/2+1)}}\cos(m_j\xi)$$

$$\bar{\Phi}_w(s) = e^{-s\tau_1^*}\sum_{j=0}^{\infty}\sum_{k=0}^{N}\frac{D_{j,k}^{(1)}\cos(m_j\xi)}{s^{(k/2+1)}} * \sum_{n=0}^{\infty} Co_{2,j}^{(1)} d_{n,j}^{(1)} s^n$$
$$= e^{-s\tau_1^*}\sum_{j=0}^{\infty}\sum_{k=-1}^{N}\frac{H_{j,k}^{(1)}}{s^{(k/2+1)}}\cos(m_j\xi)$$

$$G_{j,-1}{}^{(1)} = \sum_{k=0}^{Nk} D_{j,2k+1}{}^{(1)} E_{j,k+1}{}^{(1)}, \qquad l=-1, Nk = \mathrm{Int}\{(N-1)/2\}$$
$$G_{j,l}{}^{(1)} = \sum_{k=0}^{Nk} D_{j,2k+l}{}^{(1)} E_{j,k}{}^{(1)}, \qquad 0 \le l \le N, Nk = \mathrm{Int}\{(N-l)/2\}$$

$$H_{j,-1}{}^{(1)} = \sum_{k=0}^{Nk} D_{j,2k+1}{}^{(1)} F_{j,k+1}{}^{(1)}, \qquad l=-1, Nk = \mathrm{Int}\{(N-1)/2\}$$
$$H_{j,l}{}^{(1)} = \sum_{k=0}^{Nk} D_{j,2k+l}{}^{(1)} F_{j,k}{}^{(1)}, \qquad 0 \le l \le N, Nk = \mathrm{Int}\{(N-l)/2\}$$

where $G_{j,l}$ and $H_{j,l}$ are coefficients of Eqs.(42) and (46), respectively.

(2) For the condition that insulations are done on two opposite surfaces

$$\bar{\theta}_w(s) = e^{-s\tau_1^*}\sum_{j=0}^{\infty}\sum_{k=0}^{N}\frac{D_{j,k}^{(1)}\cos(m_j\xi)}{s^{(k/2+1)}} * \sum_{n=0}^{\infty} Co_{1,j}^{(2)} c_{n,j}^{(2)} s^n$$
$$- e^{-s\tau_2^*}\sum_{j=0}^{\infty}\sum_{k=0}^{N}\frac{D_{j,k}^{(2)}\cos(m_j\xi)}{s^{(k/2+1)}} * \sum_{n=0}^{\infty} Co_{1,j}^{(1)} c_{n,j}^{(1)} s^n$$
$$= e^{-s\tau_1^*}\sum_{j=0}^{\infty}\sum_{k=-1}^{N}\frac{G_{j,k}^{(1,2)}}{s^{(k/2+1)}}\cos(m_j\xi) - e^{-s\tau_2^*}\sum_{j=0}^{\infty}\sum_{k=-1}^{N}\frac{G_{j,k}^{(2,1)}}{s^{(k/2+1)}}\cos(m_j\xi)$$

$$\bar{\Phi}_w(s) = e^{-s\tau_1^*}\sum_{j=0}^{\infty}\sum_{k=0}^{N}\frac{D_{j,k}^{(1)}\cos(m_j\xi)}{s^{(k/2+1)}} * \sum_{n=0}^{\infty} Co_{2,j}^{(2)} d_{n,j}^{(2)} s^n$$
$$- e^{-s\tau_2^*}\sum_{j=0}^{\infty}\sum_{k=0}^{N}\frac{D_{j,k}^{(2)}\cos(m_j\xi)}{s^{(k/2+1)}} * \sum_{n=0}^{\infty} Co_{2,j}^{(1)} d_{n,j}^{(1)} s^n$$
$$= e^{-s\tau_1^*}\sum_{j=0}^{\infty}\sum_{k=-1}^{N}\frac{H_{j,k}^{(1,2)}}{s^{(k/2+1)}}\cos(m_j\xi) - e^{-s\tau_2^*}\sum_{j=0}^{\infty}\sum_{k=-1}^{N}\frac{H_{j,k}^{(2,1)}}{s^{(k/2+1)}}\cos(m_j\xi)$$

$$G_{j,-1}{}^{(1,2)} = \sum_{k=0}^{Nk} D_{j,2k+1}{}^{(1)} E_{j,k+1}{}^{(2)}, \qquad l=-1, Nk = \mathrm{Int}\{(N-1)/2\}$$
$$G_{j,l}{}^{(1,2)} = \sum_{k=0}^{Nk} D_{j,2k+l}{}^{(1)} E_{j,k}{}^{(2)}, \qquad 0 \le l \le N, Nk = \mathrm{Int}\{(N-l)/2\}$$

$$H_{j,-1}{}^{(1,2)} = \sum_{k=0}^{Nk} D_{j,2k+1}{}^{(1)} F_{j,k+1}{}^{(2)}, \qquad l=-1, Nk = \mathrm{Int}\{(N-1)/2\}$$
$$H_{j,l}{}^{(1,2)} = \sum_{k=0}^{Nk} D_{j,2k+l}{}^{(1)} F_{j,k}{}^{(2)}, \qquad 0 \le l \le N, Nk = \mathrm{Int}\{(N-l)/2\}$$

where $G_{j,l}$ and $H_{j,l}$ are coefficients of Eqs.(43) and (47), respectively.

Table A1(a) Kernel K(s) in rectangular coordinate, these coefficients in its series and common terms used in its series

	Temperature ($K_{1,n}$(s))	Heat flux ($K_{2,n}$(s))
Kernel K(s)	$\dfrac{\sinh(p\xi_n)}{\sinh\{p(\xi_2-\xi_1)\}}$	$\dfrac{p\cosh(p\xi_n)}{\sinh\{p(\xi_2-\xi_1)\}}$
Coefficients $x_{i,n}$, $y_{i,n}$	$x_{i,n} = \dfrac{1}{(2i+1)!}\xi_n^{\ 2i+1}$	$y_{i,n} = \dfrac{1}{(2i)!}\xi_n^{\ 2i}$
Common item , g_i	$g_0 = \xi_2 - \xi_1$, $g_i = \dfrac{(\xi_2-\xi_1)^{2i}}{(2i+1)!}$ $(i \ge 1)$	

Table A1(b) Kernel K(s) in cylindrical coordinate, these coefficients in its series and common terms used in its series

	Temperature ($K_{1,n}$(s))	Heat flux ($K_{2,n}$(s))
Kernel K(s) *1	$\dfrac{Z_1(\xi_n,s)}{Z_{12}(s)}$	$\dfrac{Z_2(\xi_n,s)}{Z_{12}(s)}$
Coefficients $x_{i,n}$, $y_{i,n}$ *2	$x_{i,n} = \sum_{j=0}^{i}\{-\ln(\xi_n)a_j^{\circ}b_{i-j}^{\circ}(\xi_n) + d_j^{\circ}(\xi_n)a_{i-j}^{\circ} - c_j^{\circ}b_{i-j}^{\circ}(\xi_n)\}$	$y_{i,n} = -\sum_{j=0}^{i}\{-\ln(\xi_n)e_j^{\circ}b_{i-j}^{\circ}(\xi_n) + d_j^{\circ}(\xi_n)e_{i-j}^{\circ} - f_j^{\circ}b_{i-j}^{\circ}(\xi_n)\}$
Common item, g_i *2	$g_0 = \ln(\xi_1/\xi_2)$ $\quad g_i = \sum_{j=0}^{i}\left\{b_j^{\circ}(\xi_1)b_{i-j}^{\circ}(\xi_2) + \dfrac{d_j^{\circ}(\xi_2)b_{i-j}^{\circ}(\xi_1) - d_j^{\circ}(\xi_1)b_{i-j}^{\circ}(\xi_2)}{\ln(\xi_1/\xi_2)}\right\}$ $(i \ge 1)$	

*1: Z_1, Z_2 and Z_{12} are given as:

$$Z_1(\xi_n, s) = \ln(1/\xi_n) I_0(p) I_0(p\xi_n) + X(p\xi_n) I_0(p) - X(p) I_0(p\xi_n)$$

$$Z_2(\xi_n, s) = \ln(1/\xi_n) I_1(p) I_0(p\xi_n) + X(p\xi_n) I_1(p) - \{X'(p) - I_0(p)\} I_0(p\xi_n)$$

$$Z_{12}(s) = \ln(\xi_1/\xi_2) I_0(p\xi_1) I_0(p\xi_2) + X(p\xi_2) I_0(p\xi_1) - X(p\xi_1) I_0(p\xi_2)$$

where

$$I_0(p\xi_n) = \sum_{j=0}^{\infty} \frac{s^j \xi_n^{2j}}{2^{2j}(j!)^2}, \quad I_0(p) = \sum_{j=0}^{\infty} \frac{s^j}{2^{2j}(j!)^2},$$

$$I_1(p) = \sum_{j=1}^{\infty} \frac{(2j)s^j}{2^{2j}(j!)^2}$$

$$X(p\xi_n) = \sum_{j=1}^{\infty} \frac{s^j \xi_n^{2j}}{2^{2j}(j!)^2} \sum_{m=1}^{j} \frac{1}{m}, \quad X(p) = \sum_{j=1}^{\infty} \frac{s^j}{2^{2j}(j!)^2} \sum_{m=1}^{j} \frac{1}{m},$$

$$X'(p) = \sum_{j=1}^{\infty} \frac{(2j)s^j}{2^{2j}(j!)^2} \sum_{m=1}^{j} \frac{1}{m}$$

where, I_0 and I_1 are modified Bessel functions of the first kind.
*2: The coefficients of a_j° through f_j° are summarized as:

$$a_j^\circ = \frac{1}{2^{2j}(j!)^2}, \quad b_j^\circ(\xi_n) = \frac{1}{2^{2j}(j!)^2}(\xi_n)^{2j}, \quad c_j^\circ = a_j^\circ \sum_{m=1}^{j} \frac{1}{m},$$

$$d_j^\circ(\xi_n) = b_j^\circ(\xi_n) \sum_{m=1}^{j} \frac{1}{m}, \quad e_j^\circ = (2j) a_j^\circ, \quad f_j^\circ = a_j^\circ \left(2j \sum_{m=1}^{j} \frac{1}{m} - 1 \right)$$

Table A1(c) Kernel *K*(s) in spherical coordinate, these coefficients in its series and common terms used in its series

	Temperature ($K_{1,n}$(s))	Heat flux ($K_{2,n}$(s))
Kernel K(s)	$\frac{\sinh\{p(\xi_n - 1)\}}{\sinh\{p(\xi_2 - \xi_1)\}}$	$\frac{p\cosh\{p(\xi_n - 1)\} + \sinh\{p(\xi_n - 1)\}}{\sinh\{p(\xi_2 - \xi_1)\}}$
Coefficients $x_{i,n}$, $y_{i,n}$	$x_{i,n} = \frac{1}{(2i+1)!}(\xi_n - 1)^{2i+1}$	$y_{i,n} = \frac{1}{(2i)!}(\xi_n - 1)^{2i} + \frac{1}{(2i+1)!}(\xi_n - 1)^{2i+1}$
Common item , g_i	$g_0 = \xi_2 - \xi_1$, $g_i = \frac{(\xi_2 - \xi_1)^{2i}}{(2i+1)!}$ $(i \ge 1)$	

Table A2 Kernel *K*(s) and its coefficients in its series

	Temperature (K_1(s))	Heat flux (K_2(s))
Kernel K(s)	$e^{p\xi_1}$	$pe^{p\xi_1}$
Coefficients, u_i, v_i	$u_i = \frac{\xi_1^i}{i!}$	$v_i = \frac{\xi_1^i}{i!}$

Table A3 Kernel *K*(s) and its coefficients

(1) For the condition that insulations are done on three surfaces

		Surface temperature ($K_{1,j}$(s))	Surface heat flux ($K_{2,j}$(s))
Kernel *K*(s)		$\dfrac{\cosh\{\sqrt{(s+m_j^2)}\frac{1}{L}\}}{\cosh\{\sqrt{(s+m_j^2)}(\frac{1-\eta_1}{L})\}}$	$\dfrac{\frac{\sqrt{(s+m_j^2)}}{L}\sinh\{\sqrt{(s+m_j^2)}\frac{1}{L}\}}{\cosh\{\sqrt{(s+m_j^2)}(\frac{1-\eta_1}{L})\}}$
m_j = 0 (j = 0)	**Coefficients of *K*(s) after expansion**	$x_{n,0}=\frac{1}{(2n)!}\left(\frac{1}{L}\right)^{2n}$	$y_{0,0}=0,\quad y_{n,0}=\frac{1}{(2n-1)!}\left(\frac{1}{L}\right)^{2n-1}$ (n ≥ 1)
	Coefficients Co_j	$Co_{1,0}=1$	$Co_{2,0}=\frac{1}{L}$
	Common item	$g_{n,0}=\frac{1}{(2n)!}(\frac{1-\eta_1}{L})^{2n}$	
m_j > 0 (j > 0)	**Coefficients of *K*(s) after expansion**	$x_{n,j}=\dfrac{\sum_{k=n}\frac{{}_kC_n}{(2k)!}\left(\frac{1}{L}\right)^{2k}m_j^{2(k-n)}}{\cosh(m_j\frac{1}{L})}$	$y_{0,j}=1,\quad y_{n,j}=\dfrac{\sum_{k=n-1}\frac{{}_{k+1}C_n}{(2k+1)!}\left(\frac{1}{L}\right)^{2k+1}m_j^{2(k+1-n)}}{m_j\sinh(m_j\frac{1}{L})}$ (n ≥ 1)
	Coefficients Co_j	$Co_{1,j}=\dfrac{\cosh(m_j\frac{1}{L})}{\cosh\{m_j(\frac{1-\eta_1}{L})\}}$	$Co_{2,j}=\frac{1}{L}\dfrac{m_j\sinh(m_j\frac{1}{L})}{\cosh\{m_j(\frac{1-\eta_1}{L})\}}$
	Common item	$g_{n,j}=\dfrac{\sum_{k=n}\frac{{}_kC_n}{(2k)!}(\frac{1-\eta_1}{L})^{2k}m_j^{2(k-n)}}{\cosh\{m_j(\frac{1-\eta_1}{L})\}}$	

(2) For the condition that insulations are done on two opposite surfaces

		Surface temperature ($K_{1,j}^{(l)}(s)$)	Surface heat flux ($K_{2,j}^{(l)}(s)$)
Kernel *K*(s)		$\dfrac{\sinh\{\sqrt{(s+m_j^2)}\frac{\eta_l}{L}\}}{\sinh\{\sqrt{(s+m_j^2)}(\frac{\eta_2-\eta_1}{L})\}}$	$\dfrac{\frac{\sqrt{(s+m_j^2)}}{L}\cosh\{\sqrt{(s+m_j^2)}\frac{\eta_l}{L}\}}{\sinh\{\sqrt{(s+m_j^2)}(\frac{\eta_2-\eta_1}{L})\}}$
m_j = 0 (j = 0)	**Coefficients of *K*(s) after expansion**	$x_{n,0}^{(l)}=\frac{1}{(2n+1)!}\left(\frac{\eta_l}{L}\right)^{2n+1}$	$y_{n,0}^{(l)}=\frac{1}{(2n)!}\left(\frac{\eta_l}{L}\right)^{2n}$
	Coefficients Co_j	$Co_{1,0}^{(l)}=1$	$Co_{2,0}^{(l)}=\frac{1}{L}$
	Common item	$g_{n,0}=\frac{1}{(2n+1)!}(\frac{\eta_2-\eta_1}{L})^{2n+1}$,	
m_j > 0 (j > 0)	**Coefficients of *K*(s) after expansion**	$x_{n,j}^{(l)}=\dfrac{\sum_{k=n}\frac{{}_kC_n}{(2k+1)!}\left(\frac{\eta_l}{L}\right)^{2k+1}m_j^{2(k-n)+1}}{\sinh(m_j\frac{\eta_l}{L})}$	$y_{n,j}^{(l)}=\dfrac{\sum_{k=n}\frac{{}_kC_n}{(2k)!}\left(\frac{\eta_l}{L}\right)^{2k}m_j^{2(k-n)}}{\cosh(m_j\frac{\eta_l}{L})}$
	Coefficients Co_j	$Co_{1,j}^{(l)}=\dfrac{\sinh(m_j\frac{\eta_l}{L})}{\sinh\{m_j(\frac{\eta_2-\eta_1}{L})\}}$	$Co_{2,j}^{(l)}=\frac{1}{L}\dfrac{m_j\cosh(m_j\frac{\eta_l}{L})}{\sinh\{m_j(\frac{\eta_2-\eta_1}{L})\}}$
	Common item	$g_{n,j}=\dfrac{\sum_{k=n}\frac{{}_kC_n}{(2k+1)!}(\frac{\eta_2-\eta_1}{L})^{2k+1}m_j^{2(k-n)+1}}{\sinh\{m_j(\frac{\eta_2-\eta_1}{L})\}}$,	